Applications of the Adjoint Technique to Short-Range Ensemble Forecasting of Mesoscale Convective Systems

MEI XU

Program in Atmospheric and Oceanic Sciences, University of Colorado, and National Center for Atmospheric Research, Boulder, Colorado

DAVID J. STENSRUD

NOAA/National Severe Storms Laboratory, Norman, Oklahoma

JIAN-WEN BAO

Cooperative Institute for Research in Environmental Sciences, University of Colorado, and NOAA/Environmental Technology Laboratory, Boulder, Colorado

THOMAS T. WARNER

Program in Atmospheric and Oceanic Sciences, University of Colorado, and National Center for Atmospheric Research, Boulder, Colorado

(Manuscript received 22 October 1999, in final form 26 September 2000)

ABSTRACT

The feasibility of applying a mesoscale adjoint model to the creation of an ensemble for short-range simulations of mesoscale convective systems (MCSs) is explored. Because past studies show that forecasters routinely improve upon numerical guidance and can identify mesoscale-sized areas of forecast concern with a high level of skill, it is clear that forecasters have insights into the daily weather forecast problems that exceed what can be provided by a numerical weather prediction model. Using an adjoint model, one could develop a system in which a forecaster identifies the area of forecast concern and then designs a set of rapidly produced sensitivity experiments that evaluate the influence of key atmospheric parameters on the model forecast. The output from these sensitivity experiments is then used to create ensemble members for a short-range operational ensemble forecast, which is specifically designed to investigate the forecast concern of the day.

This adjoint ensemble approach is tested for the 48-h period beginning 1200 UTC 27 May 1985, in which a long-lived MCS developed underneath a large-scale ridge. A mesoscale adjoint model is used to define the alterations to the model initial conditions necessary to evaluate the influences of key mesoscale structures, which the authors believe have a large influence on later convective development in the model. Results indicate that the adjoint technique is effective in creating the proper directional response in the model simulation.

When compared to initial condition and model physics ensembles of this event, the adjoint ensemble produces more variance than the initial condition ensemble and almost as much variance as the model physics ensemble. However, the values of the equitable threat score and the ranked probability score are better for the adjoint ensemble between 6 and 24 h than for either of the other two ensembles. These results suggest that further exploration of ensembles that incorporate the experience and expertise possessed by forecasters is warranted.

1. Introduction

Most of the perturbation techniques developed for generating medium-range ensemble forecasts have concentrated on synoptic-scale weather systems over the midlatitudes that are associated with regions of baroclinic instability (Palmer et al. 1992; Toth and Kalnay 1993; Buizza 1997; Houtekamer and Lefaivre 1997). This is a temporal and spatial scale that is well suited for numerical weather prediction, since numerical models are skillful in predicting baroclinic wave development. As the temporal and spatial scales of interest become smaller, many more instabilities and processes are known to play a significant role, at least intermittently, in the evolution of the atmosphere at a given location. The skill of numerical models in predicting the variety of mesoscale and small-scale phenomena is not well known, since our ability to observe these phenomena is

Corresponding author address: Dr. Mei Xu, Research Applications Program, National Center for Atmospheric Research, P. O. Box 3000, Boulder, CO 80307.
E-mail: meixu@ncar.ucar.edu

limited. However, if one examines summertime quantitative precipitation forecasts associated with mesoscale convective systems (MCSs), which are the result of the interactions of many mesoscale and small-scale phenomena, then it is clear that numerical models are not very skillful at predicting mesoscale processes (Heideman and Fritsch 1988).

The perturbation growth for MCSs is related to the development and evolution of convection and its associated latent heating, which are not well understood. Furthermore, parameterization schemes for convection and related processes play a significant role in the simulation of MCSs (Kain and Fritsch 1993; Wang and Seaman 1997; Stensrud et al. 2000). These schemes are simplified approximations to the behavior of actual convective clouds, have many uncertainties (Emanuel and Raymond 1992), and are strongly influenced by inaccuracies in the model initial conditions caused by the undersampling of important mesoscale features (Stensrud and Fritsch 1994; Stensrud et al. 1999). These uncertainties are likely to continue to exist, even as model grid spacing is decreased.

When these model uncertainties are combined with knowledge of the wide variety of forecast objectives found in short-range forecasting, which can vary from the evaluation of the severe weather potential to air quality issues, one must consider whether or not the techniques developed for generating medium-range ensemble forecasts are well designed for short-range ensemble forecasts. In particular, with the variety of short-range forecast objectives identified on any given day, it is unclear that a single approach for generating the ensemble initial conditions is sufficient to address all these objectives. It may be that the approach for generating ensemble initial conditions for short-range forecasting will have to incorporate many different forecast concerns. Identifying these various concerns and constructing an ensemble to provide guidance for them is a difficult problem.

One source of information that may be useful in creating short-range ensembles is the experience and skill of human weather forecasters. It is clear that forecasters routinely improve upon numerical guidance, as indicated by an examination of the skill scores for precipitation (Mostek and Junker 1989; Funk 1991). Perhaps more importantly, forecasters at the Storm Prediction Center routinely identify mesoscale-sized areas of significant severe weather threat[1] with a high level of skill (Leftwich et al. 1998; McCarthy et al. 1998). This is true even though many summertime convective events involve mesoscale processes that are difficult to predict or anticipate using current model output and observations (Doswell 1987; Rockwood and Maddox 1988; Stensrud and Fritsch 1994). Through the techniques of parameter evaluation, pattern recognition, and a knowledge of severe weather climatology, forecasters have insights into the daily weather forecast problem that far exceed what can be provided by a numerical weather prediction model alone. It seems logical that some method be developed to use these insights in the creation of short-range ensemble forecasts in order to better define the meteorological features of interest on each day. An adjoint model provides the basis for the development of such a method.

An adjoint model is the transpose of the tangent linear operator of a numerical model (Errico 1997). Over the last decade or so, adjoint models have been increasingly used in a variety of meteorological applications. The most straightforward application of adjoint models is to examine the sensitivity of the nonlinear forecast model to initial conditions or model parameters (Errico and Vukicevic 1992; Rabier et al. 1992; Langland et al. 1995; Bao and Errico 1997). The estimation of the singular vectors of a linearized model using the corresponding adjoint model has been widely used for studies of predictability, targeted observations, and medium-range ensemble forecasting (Gauthier et al. 1993; Bouttier 1993; Barkmeijer 1992; Palmer et al. 1998).

The rationale for using an adjoint model in generating ensemble forecasts is based on the fact that the adjoint sensitivity vectors are very closely related to the singular vectors of the resolvent of the tangent linear operator corresponding to the numerical model. These singular vectors provide a precise quantitative means of estimating and characterizing the growth of small perturbations over a finite period of time under very general situations (Lorenz 1965; Palmer et al. 1998). Under certain conditions, the sensitivity vector can be written as the initial singular vectors with the singular values being part of the weighting coefficients (Rabier et al. 1996). In the limit where the cost function is defined using a single model variable at a single grid point, the sensitivity vector and the initial singular vector agree precisely in structure (Palmer et al. 1998).

The calculation of both the singular vectors and the sensitivity vector (if J is defined by a norm) depends on the metric, or norm, that is used to define the inner product of two arbitrary vectors. Unfortunately, the use of different norms yields different singular vector structures and growth rates, indicating that the choice of the norm used is very important (Buizza et al. 1996; Anderson 1997; Barkmeijer et al. 1998; Palmer et al. 1998; Errico 2000). For example, one norm will filter certain instabilities (Errico 2000), while including moist processes in a norm produces large changes in singular vector structure and evolution when compared with a norm without the moist processes (Buizza et al. 1996; Ehrendorfer et al. 1999). The norm most appropriate for short-range forecasts is unknown, assuming such a norm exists in general that can be applied to the many forecast aspects that need to be evaluated on any given day.

In this study, we explore the feasibility of applying

[1] Through the issuance of 1- and 2-day outlooks and severe thunderstorm watches.

a mesoscale adjoint model to the creation of an ensemble of initial conditions for short-range simulations of MCSs. We recognize that both the large-scale environmental uncertainty, as investigated using singular vectors (Molteni et al. 1996; Buizza 1997), breeding of growing modes (Toth and Kalnay 1993), and perturbed observations (Houtekamer and Lefaivre 1997), and model uncertainty (Houtekamer and Lefaivre 1997; Stensrud et al. 2000), are important contributors to short-range ensembles. However, since it is unclear that incorporating only these uncertainies in the design of short-range ensemble systems for unlikely or infrequent events will be able to capture these events, we choose to investigate an ensemble designed to evaluate specific aspects of the weather forecast that uses an adjoint model approach.

As discussed by Errico (1997), adjoints are able to provide answers to questions such as ''how sensitive is the forecast temperature over Iowa to changes in low-level humidity over Iowa?'' By using an adjoint model, one could develop a system in which a forecaster identifies the meteorological feature of interest, and then designs a set of sensitivity experiments that evaluate the influence of key atmospheric parameters on the model forecast. The adjoint sensitivity vectors are then used to create the ensemble members for a short-range ensemble forecast. This ensemble is designed to investigate the specific feature of interest, and may have limited use for other forecast concerns on that day.

This approach is similar in philosophy to targeting adaptive observations. In the targeting approach, a verification area is chosen in which forecast errors are to be kept to a minimum, and an adjoint modeling system is used to identify the target area where analysis errors, if present, are expected to grow most rapidly and affect the verification area at a later time (Buizza and Montani 1999; Gelaro et al. 1999; Langland et al. 1999; Montani et al. 1999). Extra observations are then taken in the target area to reduce the analysis error. Presently, the norm used to identify the target area is subjectively chosen and held fixed for the experiments. The technique proposed here is similar in that a forecast target area is defined and then the sensitivity of the model forecasts within this target area is explored using an adjoint technique. The difference between this technique and targeting is that no extra observations are proposed to reduce the analysis uncertainty (although this could be done, assuming the observations could be taken and new forecasts produced before the event is expected to occur) and that the metric used to define the sensitivities is variable and chosen by the forecaster.

Admittedly, this approach is a subjective one and would be difficult to reproduce exactly at other centers if successful. But the norm selected to use in generating medium-range ensembles is also a subjective choice, as are the methods for selecting the target area in targeting adaptive observations (Reynolds et al. 2000). Another more subjective approach that has shown improvement in numerical weather prediction is the use of synthetic observations for hurricane forecasts (Fiorino et al. 1993; Goerss and Jeffries 1994). Therefore, subjective approaches can be used effectively in operational forecasting and should not be dismissed without exploring their possible value.

In evaluating the potential for an adjoint approach to create ensembles for short-range forecasting, we choose to focus upon deep convection as the feature of interest. This is because convection is the most difficult forecast aspect to predict, since it represents the outcome of all other processes in the model. We further assume that the development and evolution of deep convection is the dominant, energetically active mode in a model forecast of MCSs. The evolution of a forecast can be significantly affected if the location or timing of convective development is altered, as seen in the results of Fritsch and Chappell (1981) and Stensrud and Fritsch (1994). Although model uncertainty can be significant, as shown in Stensrud et al. (2000), we neglect it here in order to isolate the initial condition uncertainty. Buizza et al. (1999) demonstrate one technique to include model uncertainty in the generation of medium-range ensembles, while Houtekamer and Lefaivre (1997) and Stensrud et al. (2000) demonstrate different technqiues for short-range ensembles. In addition, it is possible that some model errors could be minimized through an adjoint ensemble approach if these errors are known.

In order to create an ensemble, we have attempted to produce a set of sensitivity experiments that a forecaster might have created to evaluate the severe weather threat. One benefit of this approach is that, for each sensitivity experiment the forecaster identifies, a different norm must be used. This diminishes the importance of any single norm in the ensemble forecast procedure. The hypothesis that we wish to test is: Does an ensemble created from the adjoint sensitivity vectors, with respect to known mesoscale structures that influence convective development in the model, produce a more skillful simulation with dispersion equal to, or larger than, that produced by other methods for generating short-range ensembles?

A mesoscale convective event that occurred under weak large-scale forcing for upward motion is examined in this study. An observational study of squall lines in the midwest documents that a significant number of MCSs occur in association with weak large-scale forcing (Porter et al. 1955). Previous modeling studies suggest that model sensitivities are greater for weakly forced events than strongly forced events (Stensrud and Fritsch 1994). From a forecasting perspective, weakly forced events tend to be the ones in which numerical forecast guidance is needed most (see discussion in Brooks and Doswell 1993).

The adjoint and forward models used in this study are discussed in section 2. A brief description of the event is found in section 3. The experimental design, including the selection of specific model parameters that

are used to investigate sensitivities with respect to the initial condition perturbations, is discussed in section 4. Such sensitivity analyses are important to our understanding of the mesoscale events and the numerical model alike, and the patterns produced by these sensitivity analyses are shown in section 5. Section 6 contains an exploration of the feasibility of using the adjoint model sensitivity patterns in generating initial conditions for ensemble forecasting of a MCS event. The performance of the adjoint ensemble is evaluated against two other ensemble generation techniques in section 7. The three methods are compared in terms of their ability to create spread in the ensemble members. Section 8 contains a concluding discussion.

2. The simulation system

a. The MM5 forward model

The forward model used in this study is the Pennsylvania State University–National Center for Atmospheric Research (Penn State–NCAR) nonhydrostatic mesoscale model version 5 (MM5). For details about this modeling system, refer to Dudhia (1989, 1993), Grell et al. (1994), and Warner et al. (1992). The planetary boundary layer parameterization is based on the studies of Blackadar (1979) and Zhang and Anthes (1982). For the precipitation parameterization, the Betts-Miller technique (Betts and Miller 1993; Janjic 1994) is employed. The Betts-Miller convective parameterization scheme (CPS) is frequently used by the mesoscale modeling community, and has been well tested. A simple explicit treatment of cloud microphysics is employed (Dudhia 1989). Both ice and liquid phases are permitted for cloud and precipitation, but mixed phases are not permitted. The model uses a radiation scheme in which longwave and shortwave radiation interact with the clear atmosphere, cloud, precipitation, and the ground (Dudhia 1989).

There are two computational grids (Fig. 1), with the inner and outer grids having mesh sizes of 73×73 and 96×96 points and grid increments of 25 and 75 km, respectively. The grids, each with 23 computational layers, interact during the simulation (i.e., information is passed across the interface in both directions, and each finer-grid solution replaces the coarser-grid solution in the coincident area at the end of its calculations). Vertical resolution within the planetary boundary layer (PBL) is greater than in the free troposphere above. The model top is located at 50 hPa.

The model initial conditions are generated using a standard static initialization. First-guess fields are produced by interpolating the National Centers for Environmental Prediction (NCEP) $2.5° \text{ lat} \times 2.5°$ long global analysis to the computational grids. Standard upper-air and surface observations are then used to adjust the NCEP analysis through a successive-correction type of objective analysis procedure (Benjamin and Seaman 1985). The model is initialized at 1200 UTC 27 May 1985, and 48-h simulations are produced.

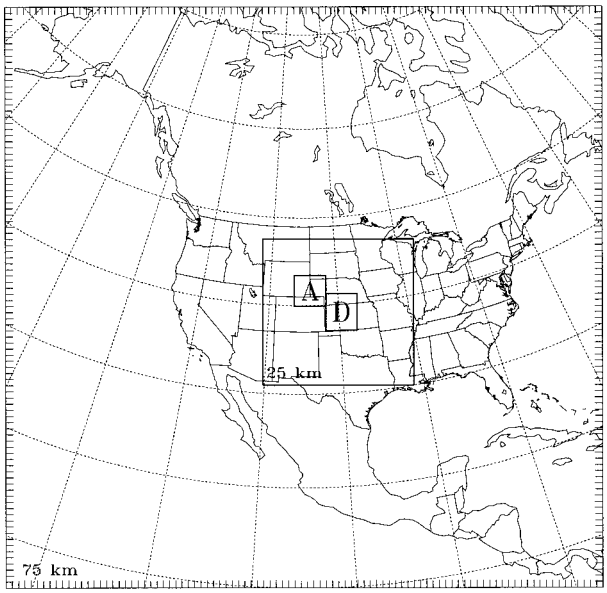

FIG. 1. Domain configurations of the MM5 simulations. The letters A and D mark the areas that are evaluated for sensitivities to various forecast aspects using the adjoint model.

b. The MM5 adjoint modeling system

The adjoint model used in this study is the MM5 Adjoint Modeling System (MM5-4DVAR) developed by NCAR. It is based on the nonhydrostatic equations of MM5, and uses the same Arakawa B grid in the horizontal and a terrain-following normalized pressure coordinate in the vertical, as in MM5. Documentation and results of some initial tests of the system can be found in Zou et al. (1995), Zou and Kuo (1996), Kuo et al. (1996, 1997), and Zou et al. (1997).

In the MM5-4DVAR, the forward MM5 is first linearized to derive the tangent linear model (TLM) of MM5. The adjoint model is then developed as the transpose of the TLM. By backward integration of the adjoint model from the forecast time to an earlier time, one can effectively compute the gradients of any MM5 forecast aspect with respect to the model control variables. The TLM and adjoint model can be used for many applications, including sensitivity analyses and four-dimensional data assimilation. In this study, the MM5-4DVAR is used for calculating sensitivity patterns.

The MM5-4DVAR used in this study is a simplified version of the full adjoint model of MM5. Dry convective adjustment is adopted, and only one mesh is used. However, we expect the dry processes to be a good approximation to the full-physics simulation before the onset of intense convective activity. Other physics within the MM5-4DVAR include a bulk PBL parameterization scheme, resolvable-scale precipitation,

and an atmospheric radiation parameterization. The domain used in the adjoint model runs is the same as the outer domain of the MM5 forward model simulations, which has 96 × 96 grid points with a horizontal grid increment of 75 km. There are 23 sigma levels in the vertical. However, the sigma levels near the surface are spaced farther apart to make the grid more compatible with the bulk PBL parameterization scheme.

The procedures for using MM5-4DVAR to conduct a sensitivity experiment, the first step in generating an ensemble, are summarized as follows.

1) Prepare the model initial and boundary conditions. The initial and lateral boundary conditions for MM5-4DVAR are prepared in the same way as the standard MM5 initial and boundary conditions are prepared (see Stensrud and Fritsch 1994).
2) Select a response function, *J*, of interest that is dependent on given model-forecast aspects and whose sensitivity is to be found. In this work, forecast aspects that are believed important for the development and evolution of MCS are selected. For example, *J* could be defined with respect to the low-level temperature at the time and location of initial convective development in the control run. In a forecast scenario, these functions are selected by the forecaster to explore the sensitivity of the model forecasts to specific meteorological features of interest.
3) Determine the adjoint form of the response function in the adjoint model. The adjoint form of the response function is added to the adjoint equations. Since this could not be done in a real-time environment, a predetermined set of response functions is needed from which the forecaster is allowed to select. However, the four-dimensional regions (space and time) over which these functions are evaluated could easily change from forecast to forecast and be selected by the forecaster.
4) Run MM5-4DVAR to find the gradients of the response function *J* with respect to the model control variables, which, in this study, are the model variables at the time of initialization. The derived gradients reflect the sensitivity of the linear model to changes in the initial conditions.

To use the sensitivity patterns to create the model initial conditions for the MM5 forward simulations, the gradient information on the adjoint model grid is interpolated to the MM5 grids. The MM5 initial conditions on both the inner and outer grids are then modified according to these sensitivity patterns, such that a desired change in the response function can be created effectively by the perturbations in the initial conditions. Details on generating the initial state perturbations in this study are given in section 4.

3. Case description

The 2-day period from 27 to 29 May 1985 contains the development and evolution of a large MCS over the Central Plains of the United States (Stensrud et al. 2000). This MCS develops under a large-scale ridge, in association with weak large-scale forcing for upward motion, and was not forecast to occur (see Meitin and Cunning 1986). While this event represents a particularly challenging forecast problem, it is also typical of the types of summertime convective events that are routinely handled by operational forecasters. Producing an accurate 24-h quantitative precipitation forecast (QPF) for such an event is extremely difficult, since many aspects of both the initiation and evolution of convection are uncertain.

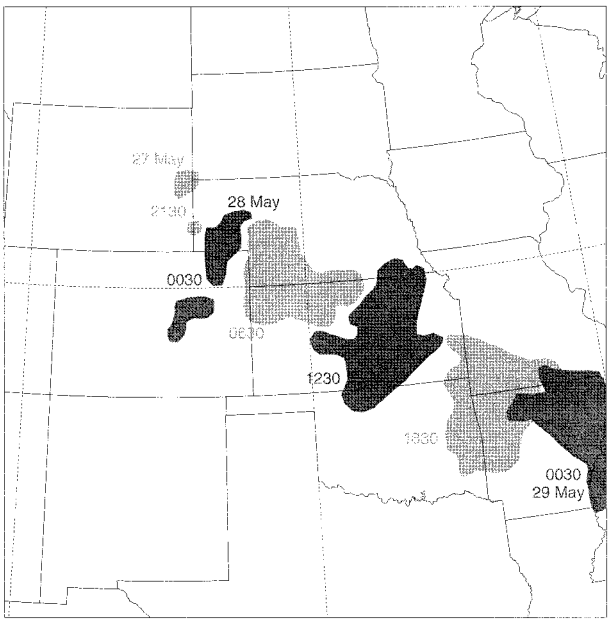

FIG. 2. Observed MCS reflectivity pattern, as indicated by the national radar summaries, from initiation at 2130 UTC 27 May through demise at 0030 UTC 29 May 1985. The MCS consists of a leading edge convective line, typically located on the southeastern flank, followed by a trailing stratiform precipitation region to the northwest.

An important feature of this May 1985 event is a convective cell that initiates in southeastern Wyoming around 1900 UTC 27 May 1985. This thunderstorm moves southeastward and slowly organizes into an MCS as it enters into northwestern Kansas. This MCS continues to move southeastward over the next 18 h as it crosses Kansas, skirts the far northeastern corner of Oklahoma, and moves into Arkansas (Fig. 2). More details of the event are given in Stensrud et al. (2000). The MM5 simulation of the event has been shown to be sensitive to model physics options and initial conditions (Stensrud et al. 2000).

4. Experimental design

a. Selection of the response functions

The choice of a response function, *J*, depends on the specific meteorological feature of interest and the fore-

caster's understanding of how the atmospheric processes associated with this feature evolve in the atmosphere and model. For organized convection, the idea is to select the mesoscale structures that are believed to have a large influence on both the initial and later convective development in the model. This selection process is a crucial part of an adjoint-based ensemble approach, since it is possible to select parameters that are not strongly related to the feature of interest. Fortunately, the techniques of parameter evaluation, pattern recognition, and a knowledge of climatology are very beneficial to this selection process, just as they are for the forecast process.

Two regions of interest are investigated for the MCS event of May 1985: the region of convective initiation in the control run, and the region into which the MCS moves in the control run (areas A and D, respectively, in Fig. 1). These regions are chosen because it is natural to assume that larger sensitivities are produced by the forecast aspects in the modeled atmosphere near the regions of convective development and evolution in both space and time as shown in the control simulation. Each of these two areas cover about 6×6 coarse-mesh grid points and have horizontal dimensions of 450×450 km. The parameters selected for testing within these regions are: low-level (within the PBL) moisture, low-level temperature, midlevel resolvable-scale vertical motion, low-level meridional wind speeds, and low-level moisture divergence. The response functions are defined as the mean of the variable in the area instead of the value at one grid point. An area, instead of a point, is chosen to define the response function in order to explicitly reflect our uncertainty in the precise location where the sensitivity to a given parameter is largest. It is our belief that an operational forecaster would produce a set of sensitivity experiments that resemble what we have chosen, and perhaps even improve upon them.

Each adjoint solution describes the sensitivity of a single forecast aspect with respect to perturbations of all initial state fields. However, as pointed out by Errico and Vukicevic (1992), the adjoint solution does not describe the entire impact throughout the length of the forecast of making a perturbation in the initial state fields. That is, the adjoint solution tells us how initial state perturbations affect J at a particular time and place, but describes nothing about the effect of the perturbations on all the other aspects of the forecast. The total effect of the perturbations on the model simulation remains unknown from the adjoint runs.

Since our purpose is to efficiently create an ensemble of model solutions that are guided by forecaster input, the uncertainty in the total effect of the perturbations should not have a severe impact on our results. On the other hand, if several forecast aspects are controlled by the same physical processes, they may yield similar characteristics of sensitivity. This would limit the usefulness of the resulting ensemble forecasts. However, if the model sensitivities to distinctly different forecast aspects are similar, then this may imply a specific response in the behavior of the atmosphere, which would be useful information from a forecast perspective. It is also possible that a poor choice for one of the forecast aspects to be evaluated could lead to an improved forecast ensemble. Even with all these unknowns, it is hypothesized that an ensemble created from selected adjoint sensitivity vectors can produce a more skillful simulation with dispersion equal to, or larger than, that produced by other methods for generating short-range ensembles.

b. Creating initial condition perturbations

Once a response function is selected, the adjoint model run produces the gradient fields of the response function with respect to the initial fields of wind (u and v), temperature (T), relative humidity (q), and the perturbation pressure (pp). The initial conditions at a grid point, (u_o, v_o, T_o), are then perturbed by an amount proportional to the gradient values at the grid point to give the perturbed initial conditions, (u_{op}, v_{op}, T_{op}); that is,

$$u_{op} = u_o + (\pm c_u)\left.\frac{\partial J}{\partial u}\right|_{t=0},$$

$$v_{op} = v_o + (\pm c_v)\left.\frac{\partial J}{\partial v}\right|_{t=0}, \quad \text{and}$$

$$T_{op} = T_o + (\pm c_T)\left.\frac{\partial J}{\partial T}\right|_{t=0}, \tag{1}$$

where c_u, c_v, and c_T are constant coefficients for the three variables in a perturbation experiment. In principle, the values of c_u, c_v, and c_T should be chosen such that the maximum perturbation sizes in the initial condition fields are comparable to the magnitudes of analysis errors. The plus/minus signs indicate the two opposite directions of perturbations. From one adjoint sensitivity experiment, two sets of symmetric initial condition perturbations, targeted at increasing and decreasing the response function, are generated. The specified perturbations are included in the initial conditions directly without using data assimilation techniques; this is justifiable as long as the perturbations are a possible realization of the analysis errors. The initial state variables for q (mixing ratio) and pp (perturbation pressure) are not perturbed in the perturbation runs, since pp is diagnosed at model initialization and there is no well-defined uncertainty in the analyses of q.

It can be shown (Errico 1997) that the perturbations defined in (1) are the smallest perturbations to the model input that can produce a desired change of J. Therefore, by using the initial perturbations defined by (1), a change in J is created using the most efficient perturbation patterns.

TABLE 1. List of the adjoint experiments.

Experiment name	Parameter modified
J1	$J_1 = q$ at 9 h in the PBL over A
J2	$J_2 = T$ at 9 h in the PBL over A
J3	$J_3 = u$ wind component at 9 h in the PBL over A
J4	$J_4 = w$ at approximately 850 mb at 9 h over A
J5	J_5 = moisture divergence at 9 h in the PBL over A
J6	$J_6 = \upsilon$ wind component at approximately 850 mb at 18 h over D
J7	$J_7 = w$ at approximately 850 mb at 18 h over D
J8	$J_8 = q$ in the PBL at 18 h over D
J9	$J_9 = T$ in the PBL at 18 h over D

c. The adjoint ensemble

Using the two perturbed initial conditions given in (1), and keeping the model physics constant, two nested-grid MM5 simulations are conducted for each adjoint sensitivity experiment selected. The initial state perturbations are interpolated from the coarse grid to the inner fine grid in order to provide initial conditions for the nested-grid run. Since a total of nine sensitivity experiments are chosen in this study, 18 perturbation simulations (one positive and one negative from each sensitivity experiment) are produced to create the adjoint ensemble (see Table 1), which also includes the control run. The lateral boundary condition for the coarse grid is not perturbed in the simulations. Therefore, the influences of the domain lateral boundaries are not considered, which is justifiable when the domain is large and the integration time is relatively short.

The maximum perturbation sizes in the initial conditions are set to 8 m s^{-1} for u and υ, and 4 K for T. While these maximum values may seem large, we believe that they are reasonable. Hoecker (1963) reports on observations from a pilot balloon network over the central United States that show mesoscale wind field structures, such that errors in wind speeds of 8 m s^{-1} are easily produced between the standard upper-air stations. However, in general, little is known about the observational uncertainties on the mesoscale. Thus, the adjoint model sensitivity patterns are used as a guide to defining the maximum perturbation sizes. The sensitivity patterns typically produce alternating ribbons of positive and negative gradients whose structures would be hard to identify in the present upper-air observational network (Fig. 3). Regions with the maximum perturbation sizes are small and often located between upper-air observation sites for this case, with much smaller perturbation values typically produced at the observation sites. Therefore, we have chosen the perturbation sizes to be as large as possible, yet still produce relatively small (2 m s^{-1} and 1.5 K) perturbations over most of the perturbed areas. It is clear that more research is needed into understanding the analysis uncertainty on the mesoscale, and we recognize that the perturbations used may be an overestimate of the mesoscale analysis uncertainty. However, we do not believe that this overestimate significantly influences the results presented.

d. Adjoint model performance

The validity of the TLM in a four-dimensional variational data assimilation (4DVAR) system depends on how good the linearity approximation is, for the magnitude of perturbation considered, for a given model. Previous studies using a mesoscale model (e.g., Vukicevic 1991; Errico et al. 1993) have shown that, for initial perturbation of moderate sizes and evolution range of 1–1.5 days, the TLM is a good approximation to its nonlinear counterpart. But many processes are simulated in a nonlinear model that are not linearized, and this can lead to deficiencies in adjoint techniques (Buizza and Montani 1999). Thus, the linearity approximation of the TLM in MM5-4DVAR is briefly examined in this section, for the given response functions and perturbation sizes.

More importantly, two other sources of error may affect the performance of the MM5-4DVAR system: the exclusion of certain model terms in the linearization process and the approximation of the true basic state about which the linearization is performed (Errico et al. 1993). Since the MM5-4DVAR is not the exact adjoint model to the MM5 used in the ensemble simulations, one would like to verify that the gradients and initial conditions created by MM5-4DVAR produce the correct directional shift in the response functions in the full-physics MM5 simulations. As discussed in section 26, the MM5-4DVAR is derived from a simplified, nonlinear MM5, which is used as the forward model in the MM5-4DVAR system. There are two major differences between the simplified MM5 used in MM5-4DVAR and the full-physics MM5 used in the ensemble simulations. One difference is in the physics schemes. The MM5-4DVAR uses simplified physics schemes, which are only approximations to the MM5 physics. The other difference is in the grid configuration, where the MM5-4DVAR uses only a single coarse grid while the MM5 simulations are nested-grid runs. The MM5-4DVAR grid also has a coarser vertical resolution inside the PBL than does MM5.

Using adjoint experiment J2 (Table 1) as an example, the effectiveness and limitations of the adjoint technique in creating the correct shift in the response function is examined. The response function defined in experiment J2 is the low-level temperature at 9 h over area A, the area of initial convective development in the control simulation. As discussed in the previous sections, the adjoint model run produces the gradient fields of J_2 with respect to the initial state variables. Two perturbed initial conditions are defined using (1): one designed to decrease J_2 in the forward simulation (MINUS), and the other designed to increase J_2 in the forward simulation (PLUS).

We first examine how the simplified forward MM5

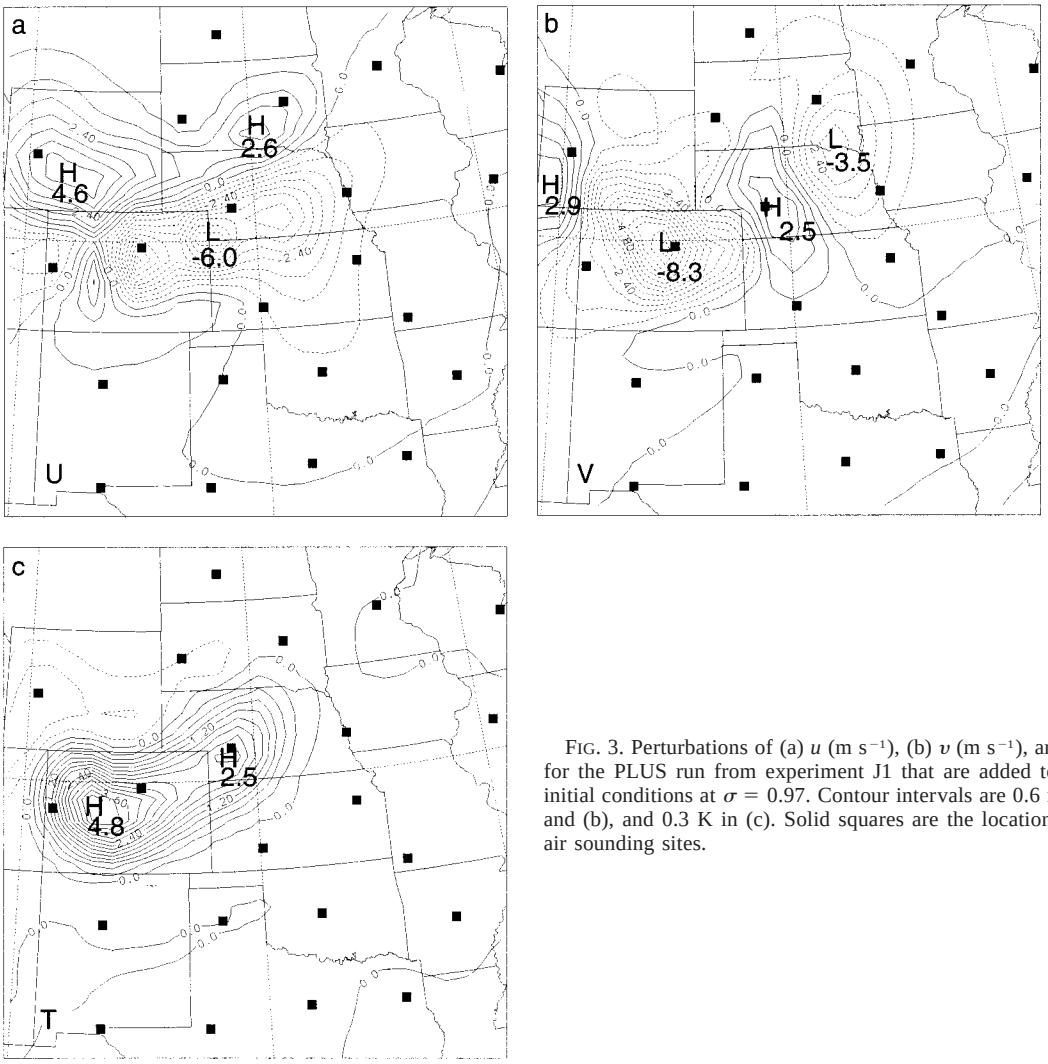

FIG. 3. Perturbations of (a) u (m s^{-1}), (b) v (m s^{-1}), and (c) T (K) for the PLUS run from experiment J1 that are added to the MM5 initial conditions at $\sigma = 0.97$. Contour intervals are 0.6 m s^{-1} in (a) and (b), and 0.3 K in (c). Solid squares are the locations of upper-air sounding sites.

in the MM5-4DVAR system responds to the two perturbed initial conditions. When the adjoint perturbations are inserted into the model initial conditions and the simplified MM5 is used, the low-level temperature is increased or decreased by about 1–4 K from the values in the control run (Fig. 4). The maximum changes in the PBL temperature over A occur at 9 h of the simulation time, which is the targeted perturbation time. The sizes of reduction and increase differ by no more than 30%, indicating that the system is approximately linear with respect to the perturbations in the model initial state. These results suggest that the linearity assumption in MM5-4DVAR is acceptable, given initial condition perturbations in the specified size range.

However, the ensemble simulations are performed using the full-physics MM5. The response function, J_2, from the control and perturbed simulations using the nested-grid, full-physics MM5 forward model is different from that of the simplified MM5 in the adjoint system (cf. Figs. 4 and 5). Comparison of the control runs show that the low-level temperatures in the control run using the full-physics MM5 are much higher than those in the control run using the simplified MM5, likely owing in part to the greater vertical resolution in the PBL with the full-physics MM5. In both versions of MM5, the maximum changes in the PBL temperature over A occur around 9 h, the targeted perturbation time (Fig. 5). In addition, the changes in low-level temperature have the correct signs in both the MINUS and PLUS runs, which proves that the initial conditions created by MM5-4DVAR are able to create the correct directional changes in the MM5 simulations. However, the sizes of reduction and increase of low-level temperature in the perturbation runs are different. The size of the temperature reduction in the MINUS run is about three times as large as that of the temperature increase in the PLUS run. Since the initial perturbations in the two runs are equal in magnitude (with opposite signs), this result is an indication of the nonlinearity in the full-physics model runs with respect to the given initial con-

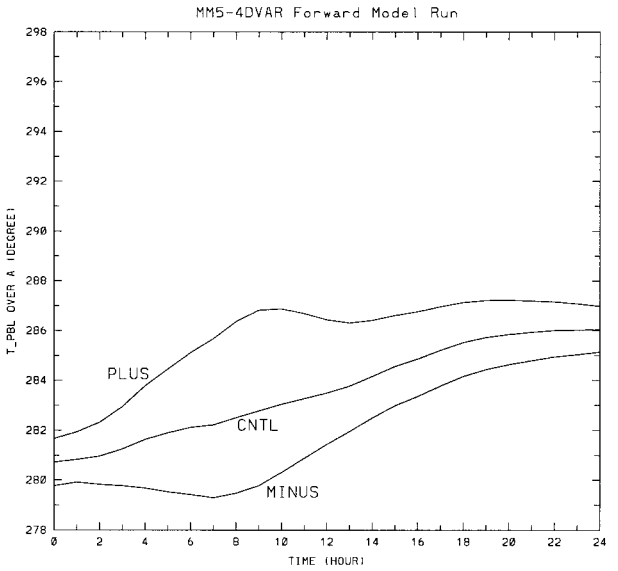

FIG. 4. The PBL temperatures over area A (K) from experiment J2 as functions of simulation time (h) in the forward simulations using the single-mesh, simplified MM5. PLUS (MINUS) indicates the simulation using initial conditions that aims to increase (decrease) J_2.

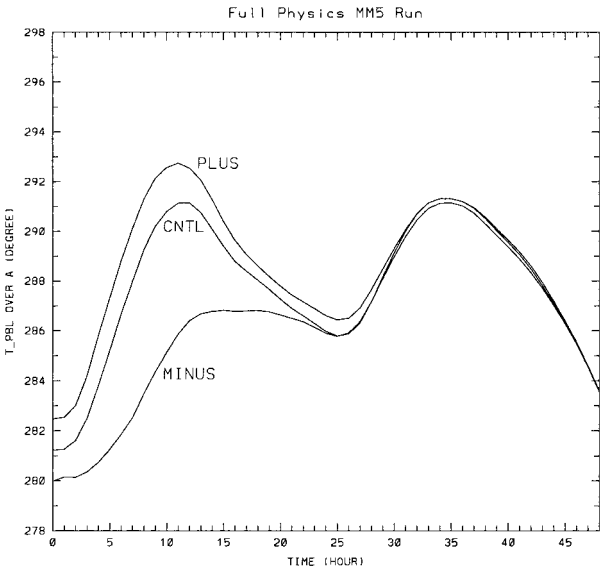

FIG. 5. As in Fig. 4 except using the nested-grid, full-physics MM5. Note that a longer simulation time is shown in Fig. 5 than in Fig. 4.

dition perturbations. Further tests show that when the perturbation sizes are reduced by half, the nonlinearity is reduced but still exists (not shown).

Therefore we may conclude that, for the given sizes of initial condition perturbations, the TLM in MM5-4DVAR is a good approximation to the simplified MM5, while there is only limited validity of the linearity assumption in the full-physics MM5. However, based on the simplified adjoint model, one can generate initial condition perturbations that perturb a forecast aspect of interest in the full-physics MM5. When paired-up MM5 simulations are conducted using symmetric perturbations of the initial conditions, the results of these perturbations are not necessarily symmetric.

Further examinations show that, in all of the perturbation runs conducted in this study, the response functions in the full-physics MM5 are perturbed effectively toward the correct direction (not shown). The above conclusions from the low-level temperature experiment (J2) apply to all of the adjoint perturbation runs. Though a more accurate adjoint model may reduce this asymmetry, assuming that the asymmetry is not due to nonlinearity, we consider that the current MM5-4DVAR is acceptable for our purposes. Thus, we proceed to examine the results of the sensitivity experiments using the full-physics MM5.

5. Sensitivity patterns

Using the Betts-Miller CPS and the control initial conditions, the MM5 simulation of the MCS event produces two well-organized convective systems, one that initiates around 9 h near the Wyoming–South Dakota border, and the other initiates in western Nebraska (region A in Fig. 1) around 12 h. The northern system moves nearly due eastward, while the southern system moves southeastward. The southeastward-moving MCS enters Kansas between 12 and 24 h and produces precipitation in both Kansas and Oklahoma by 27 h (Fig. 6). This MCS dissipates by 33 h.

The adjoint sensitivity patterns, that is, the gradient fields of the response function with respect to the initial conditions, are determined by the physical processes that propagate a set of infinitesimal initial disturbances and affect the model simulation at a later time. Therefore, analyses of the adjoint sensitivity patterns can sometimes be instructive in understanding these complicated physical processes. This understanding would likely assist forecasters in interpreting the output from the adjoint ensemble. The sensitivity patterns from J2, J5, and J9 (Table 1) are presented as examples of the adjoint sensitivity analysis. Since the gradients are calculated using the simplified adjoint model, some processes, such as moist convective adjustment, are not included.

a. Experiment J2: Low-level temperature over A at 9 h

The horizontal fields of the *u* and *T* sensitivities show that values of the gradients, positive or negative, are found in the regions relatively close to the response region A (Fig. 7). There is little structure near the domain boundaries, suggesting that the domain is large enough that the lateral boundaries do not seriously affect the model simulations. In terms of vertical structure, larger gradients of sensitivity are found in the lowest few model levels that are within and immediately above

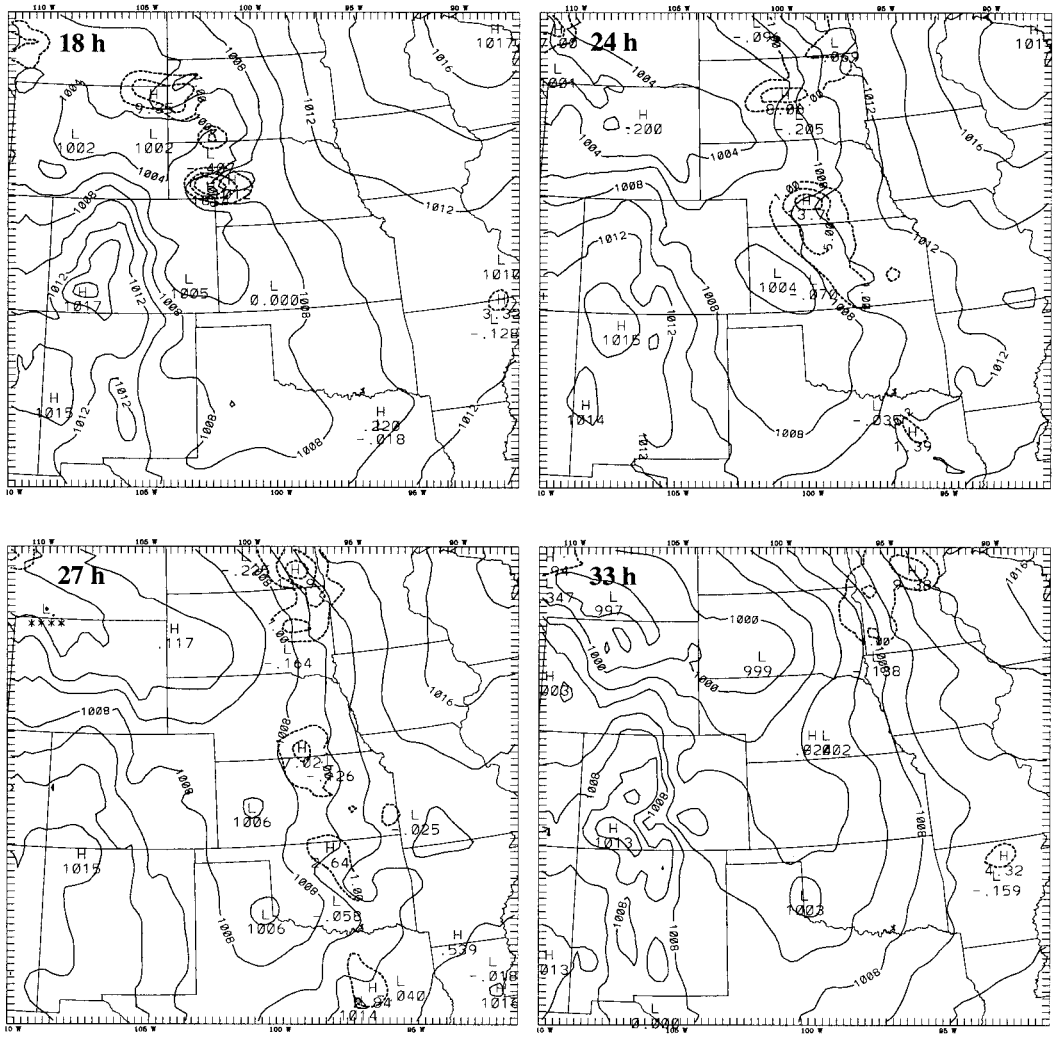

FIG. 6. The modeled 3-h precipitation (mm; dashed lines) and SLP fields (hPa; solid lines) from the control simulation at 18, 24, 27, and 33 h. The precipitation fields are contoured at 1, 5, and 10 mm, and the SLP at interval of 2 hPa.

the PBL. The magnitudes of the gradients at $\sigma = 0.98$ are about an order of magnitude larger than those at $\sigma = 0.37$ (Fig. 7). In addition, there are alternating positive and negative centers in the horizontal planes. At $\sigma = 0.98$, the distance between the positive and negative centers is about 400 km. This distance increases with height, and at $\sigma = 0.79$ it is about 700 km. At upper levels, the gradient fields exhibit asymmetric ringlike structures, with the center of the rings shifted away from the center of the response area and the radii of the rings between 1000 and 2000 km.

At $\sigma = 0.98$, the values of the T sensitivity are mostly positive and concentrated in a region of about 500 km in size. This is not surprising, considering that the response function is the low-level temperature near the region only 9 h later. A negative center appears above the PBL near area A (Fig. 7d), indicating that the midlevel cooling over the region at the initial time results in warming in the low-level temperature over the same region 9 h later. The relationship between the T and u sensitivity fields shows that the maximum u sensitivities occur in the horizontal region where the T sensitivity is changing most rapidly, with warming occurring to the left of the wind direction. This suggests that the combined effect of the sensitivity field is largely to create a modified geostrophic wind field. In midlevels, the net result is an enhanced geostrophic westerly flow in Wyoming and Nebraska, and an enhanced geostrophic easterly flow in both Kansas and Colorado, and North Dakota and Montana. Modification of the geostrophic wind is one method by which to produce long-lived changes in a model simulation.

Although at each horizontal level there are positive and negative values of the u and v sensitivity, the dominant signs of the two gradients at midlevels are positive. This indicates that the effect of increasing the southwesterly wind at the initial time is to increase the low-level temperature at 9 h over region A. This may be

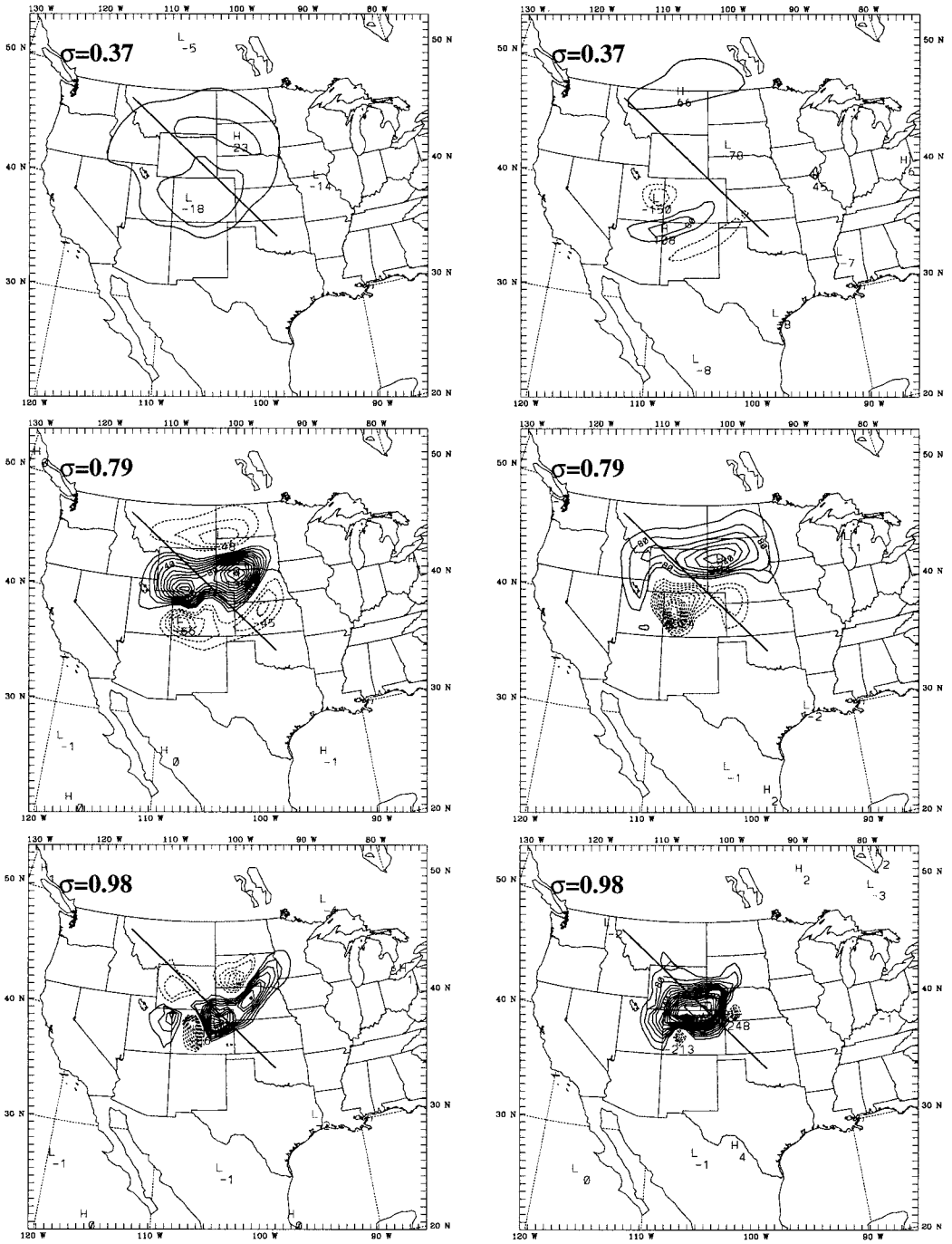

FIG. 7. Adjoint sensitivity patterns from experiment J2 showing the horizontal fields of the gradients of J_2 with respect to the initial fields of (left panels) u and (right panels) T at $\sigma = 0.37$, 0.79, and 0.98. The values shown are multiplied by a factor of 1000. The contour intervals are 10 for u sensitivity and 40 for T sensitivity, corresponding to 0.01 K s m^{-1} and 0. 04, respectively.

explained by the horizontal distribution of the temperature field. At the midlevels, the air in the southwestern part of the domain is warmer. Increasing the wind would result in enhanced warm-air advection from the southwest toward the response region, leading to increases in PBL temperatures through entrainment.

While the largest magnitudes of T sensitivity are found at the lowest model level, the largest u sensitivity is found at the level immediately above the PBL. This result is more clearly seen in the vertical cross sections of the sensitivity fields (Fig. 8). The vertical sensitivity structures show slanted features of positive and negative

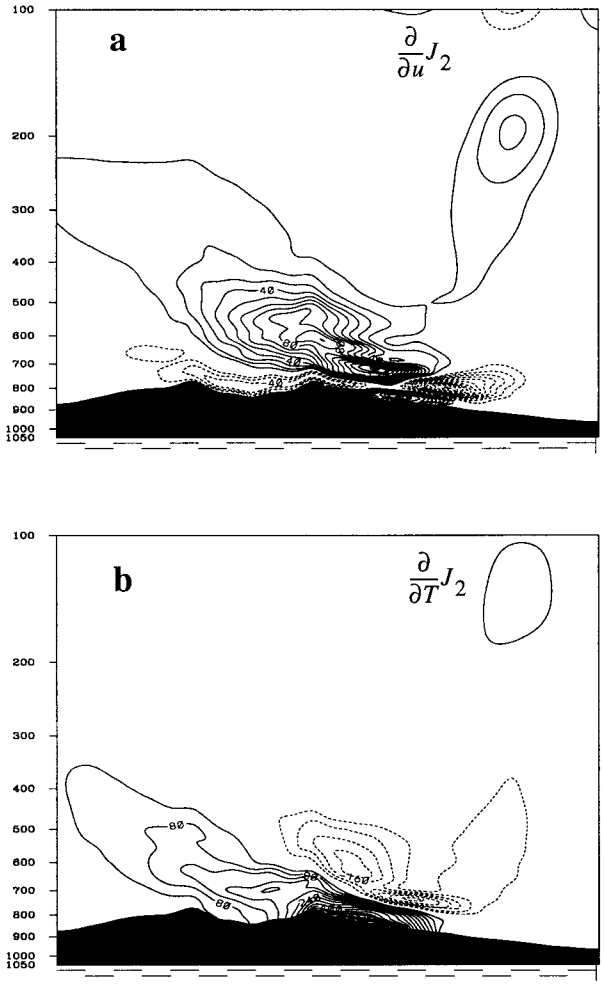

FIG. 8. Vertical cross sections of the adjoint gradients from experiment J2. (a) *u* sensitivity and (b) *T* sensitivity. The location of the vertical cross section on the horizontal plane is marked by the straight lines in Fig. 7. The contour intervals are 10 for *u* sensitivity and 40 for *T* sensitivity corresponding to 0.01 K s m^{-1} and 0.04, respectively.

gradients stacked upon each other, with little amplitude above 500 hPa.

b. Experiment J5: Low-level moisture divergence over A at 9 h

Since low-level moisture divergence is directly related to upward heat transfer and cloud formation, it is considered as a forecast aspect that may have an important effect on the subsequent convective development and evolution. Experiment J5 uses the PBL moisture divergence in region A prior to convective development (at 9 h) as the response function. The *u* and *T* sensitivity fields again have alternating positive and negative centers in the horizontal planes (Fig. 9). However, the dimensions of these patterns are smaller than those in the J2 experiment (see Figs. 7, 8). In addition, the scales of the patterns do not increase with height and the gradients of J_5 do not show a dramatic decrease in magnitude with height. This indicates that the initial condition fields at upper levels, as well as those at lower levels, have significant control over the PBL moisture divergence in the low levels within area A 9 h later.

For this forecast aspect, the relationship between *T* and *u* sensitivity fields appears to be highly ageostrophic. Since the response function J_5 is related to the horizontal derivatives of the control variables, these sensitivity structures may correspond to gravity waves. This hypothesis is supported by an analysis of the evolution of this feature in the model. Hourly model output shows that the wavelike structure moves eastward at 28 m s^{-1}, in good agreement with the speed of 24 m s^{-1} calculated from the gravity wave model of Eom (1975) using a sounding from the nearest model grid point. The modifications to the thermodynamic structure of the atmosphere in this region, produced from the perturbation derived from the adjoint sensitivity fields, includes the development of a low-level stable layer and a midlevel neutral layer. These conditions agree well with those needed to develop trapped gravity waves (Lindzen and Tung 1976). The upright orientation of the modeled vertical motion field associated with the wave is characteristic of a trapped gravity wave, providing further support for the gravity wave interpretation of this particular sensitivity field.

This analysis indicates that small-scale, ageostrophic features, possibly gravity waves, may play an important role in producing the directional shift of particular aspects in the model simulations that are used to create an ensemble for short-range forecasting. This result may seem surprising, since many initialization routines for numerical weather prediction models have historically attempted to filter out gravity waves (Baer and Tribbia 1977; Daley 1979; Temperton and Williamson 1979). Yet it is well known that gravity waves often play a role in the development and evolution of convection (Uccellini 1975; Lindzen and Tung 1976; Stobie et al. 1983; Einaudi et al. 1987; Zhang and Fritsch 1988; Powers and Reed 1993; Stensrud and Fritsch 1994). Thus, the addition of gravity waves to the model initial conditions in order to generate an ensemble is deemed a potentially realistic alteration to the initial conditions.

c. Experiment J9: Low-level temperature over D at 18 h

The response function in J9 is defined similarly to that in J2, except at a different region in time and space (Table 1). Region D is an area that may significantly affect the southeastward-moving MCS, seen in the control run, after 18 h. Horizontal and vertical cross sections of the *u* and *T* sensitivity fields show that the maximum magnitudes of the gradients are slightly smaller than those in experiment J2, while the dimensions of the sensitivity structures are larger than those in J2 (Fig. 10). This indicates an increase in the size of the influence

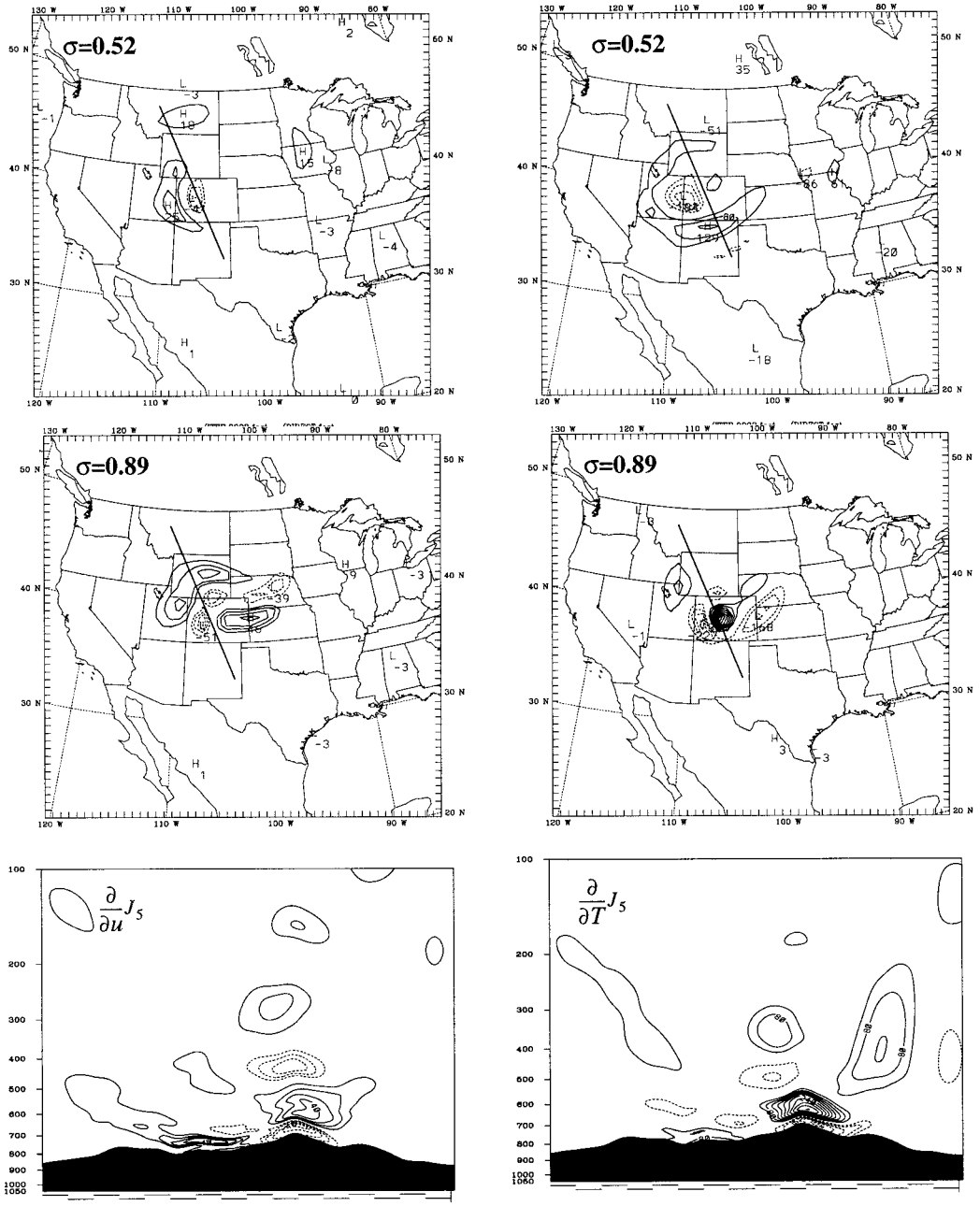

FIG. 9. Adjoint sensitivity patterns from experiment J5: the horizontal and vertical cross sections of the (left panels) u sensitivity and (right panels) T sensitivity. The horizontal cross sections are at $\sigma = 0.52$ and 0.89. Location of the vertical cross section is marked by the straight lines on the horizontal plane. The contour intervals are 10 for u sensitivity and 40 for T sensitivity, corresponding to 0.01g kg^{-1} km^{-1} and 0.04 m s^{-1} g kg^{-1} km^{-1} k^{-1}, respectively.

area of the initial perturbations for response functions that are defined at later times. Again, the largest gradients are found in the lowest few model levels within and immediately above the PBL. The magnitudes of the gradients decreases with height above the PBL, while the scales of the patterns increase with height. The larger gradient values are found in the northwest with respect to the response region (upstream), with slanted structures in the vertical tilting upward to the northwest.

These sensitivity patterns do not appear to be geostrophically balanced, but still are related to the large-scale flow pattern. The u sensitivities in Nebraska suggest a convergence zone, while a divergence pattern is seen in southern Kansas and Oklahoma. When combined with the T sensitivity field, and knowing that the low-level winds are northeasterly in Nebraska, the net result of these sensitivity fields is the contraction and movement of the warm region southward over time. The

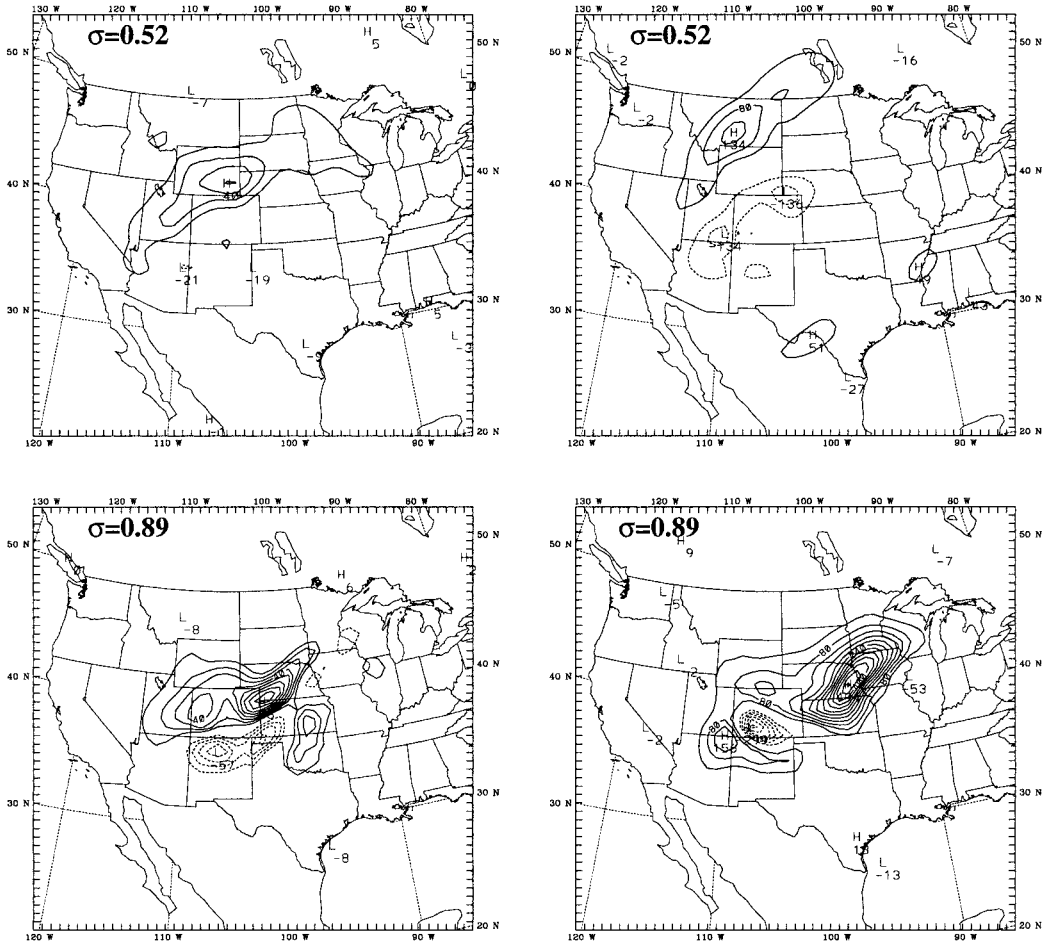

FIG. 10. Adjoint sensitivity patterns from experiment J9: horizontal cross sections of the (left panels) *u* sensitivity and (right panels) *T* sensitivity at $\sigma = 0.52$ and 0.89. The contour intervals are 10 for *u* sensitivity and 40 for *T* sensitivity, corresponding to 0.01 K s m^{-1} and 0.04, respectively.

lack of a vertical coherence in the sensitivity patterns suggests that deep ageostrophic circulations do not play a large role for this particular forecast aspect. The model sensitivities to these response functions are now examined.

6. Sensitivity of the MCS simulations to changes in the response function

The purpose of using the various perturbed initial conditions in the simulations of a MCS is to create directional disturbances in selected forecast aspects that may significantly affect the subsequent simulation of the event of interest. The responses of the full-physics MM5 simulations to the adjoint sensitivity-based initial condition perturbations, and thus the disturbances in the forecast aspects, are examined in this section. A more quantitative evaluation of the dispersions and the performance of the adjoint ensemble are given in section 7.

a. Sensitivity of the MCS simulations to low-level temperature over A at 9 h (J2)

It has already been shown how the simulated low-level temperature at area A responds to the prescribed initial condition changes (Fig. 5). The maximum changes in the simulated low-level temperature appear near 9 h, and large differences in low-level temperature between the two perturbation runs last for approximately 10 h. With maximum initial wind perturbations of 8 m s^{-1} and initial temperature perturbations of 4 K, the maximum change in PBL temperature is about 4 K.

The sea level pressure (SLP) fields respond to the initial conditions quickly and show significant differences between the two runs beginning just 3 h after the model initialization (not shown). When J_2 is increased (PLUS run), the model forecast produces two MCSs, as in the control run (cf. Figs. 6, 11). However, in the PLUS run the northern system is much stronger and the southeastward-moving MCS is slightly weaker than in the control run (Fig. 11). When J_2 is decreased (MINUS

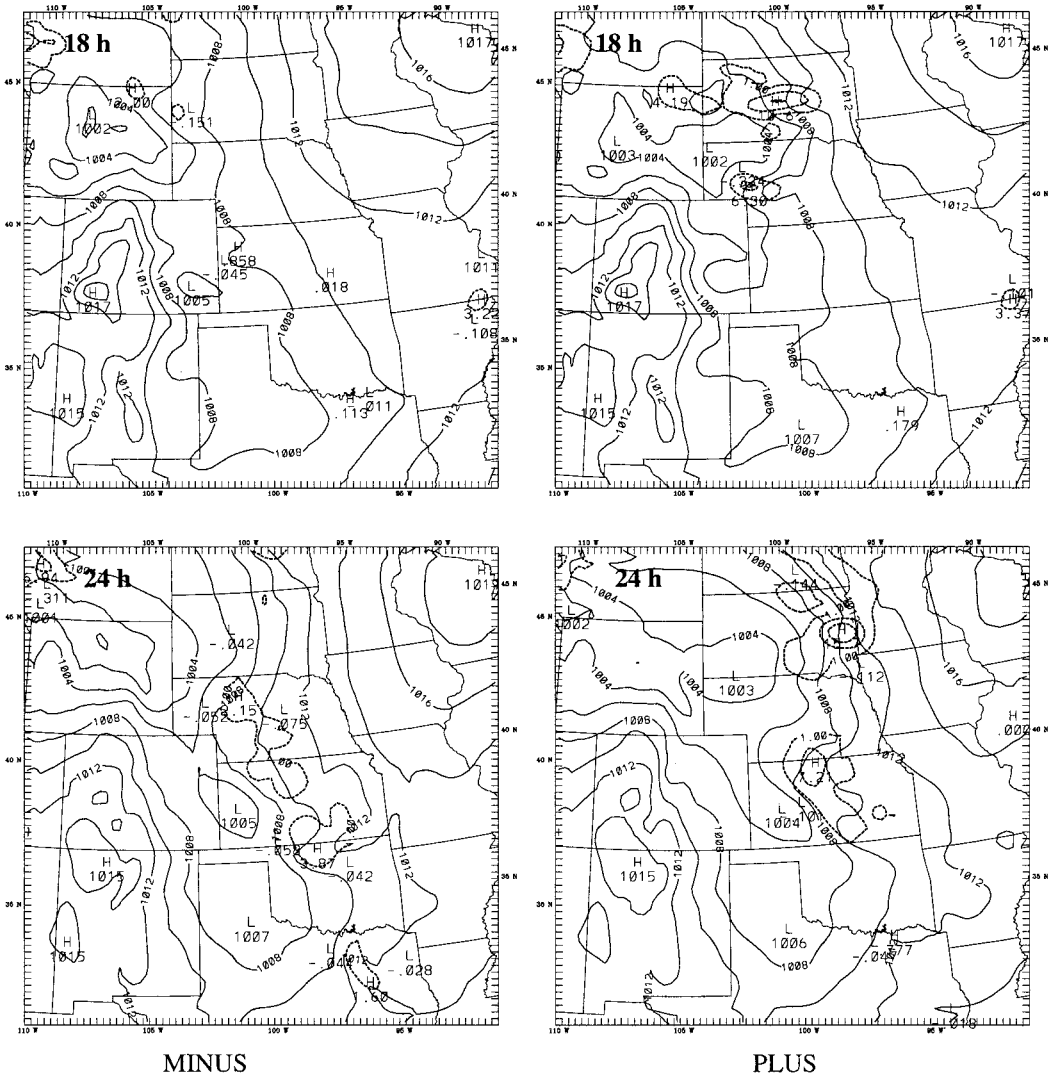

FIG. 11. Modeled 3-h precipitation (mm; dashed) and SLP fields (hPa; solid) from perturbation simulations valid at 18 and 24 h, using initial conditions from experiment J2. (Left) MINUS run; (right) PLUS run. The contour intervals are the same as in Fig. 6.

run), the simulation produces an entirely different scenario. Initially, there are still two regions of convective development at around 9–12 h. However, the northern system dissipates by 18 h, and the southern system occurs farther south, in eastern Colorado instead of western Nebraska. This southern system moves southeastward and crosses Kansas and Oklahoma earlier than that in the control run. The precipitation intensity over the Nebraska and Kansas region increases by more than 100% from the MINUS run to the PLUS run. The locations of convective activity are also obviously different in the two runs, with differences apparent by 9 h into the simulations.

A similar experiment is J1, in which the low-level moisture over area A at 9 h is perturbed. When J_1 is increased (PLUS run), the model forecast produces a much stronger southeastward-moving MCS than that in the control run. A decreased J_1 (MINUS run) causes the southeastward-moving MCS to become weaker (not shown).

b. Sensitivity of the simulations to low-level moisture divergence over A (J5)

The SLP fields and 3-h precipitation rates of the two simulations using initial conditions based on adjoint experiment J5 show that both perturbed simulations are very different from the control run and from each other (Fig. 12). As with J2, when the low-level moisture divergence at 9 h over A is decreased (i.e., convergence enhanced), the southeastward-moving MCS becomes much stronger, while the northern system dissipates after 18 h. When the low-level moisture divergence is enhanced (i.e., convergence reduced), the southeastward-

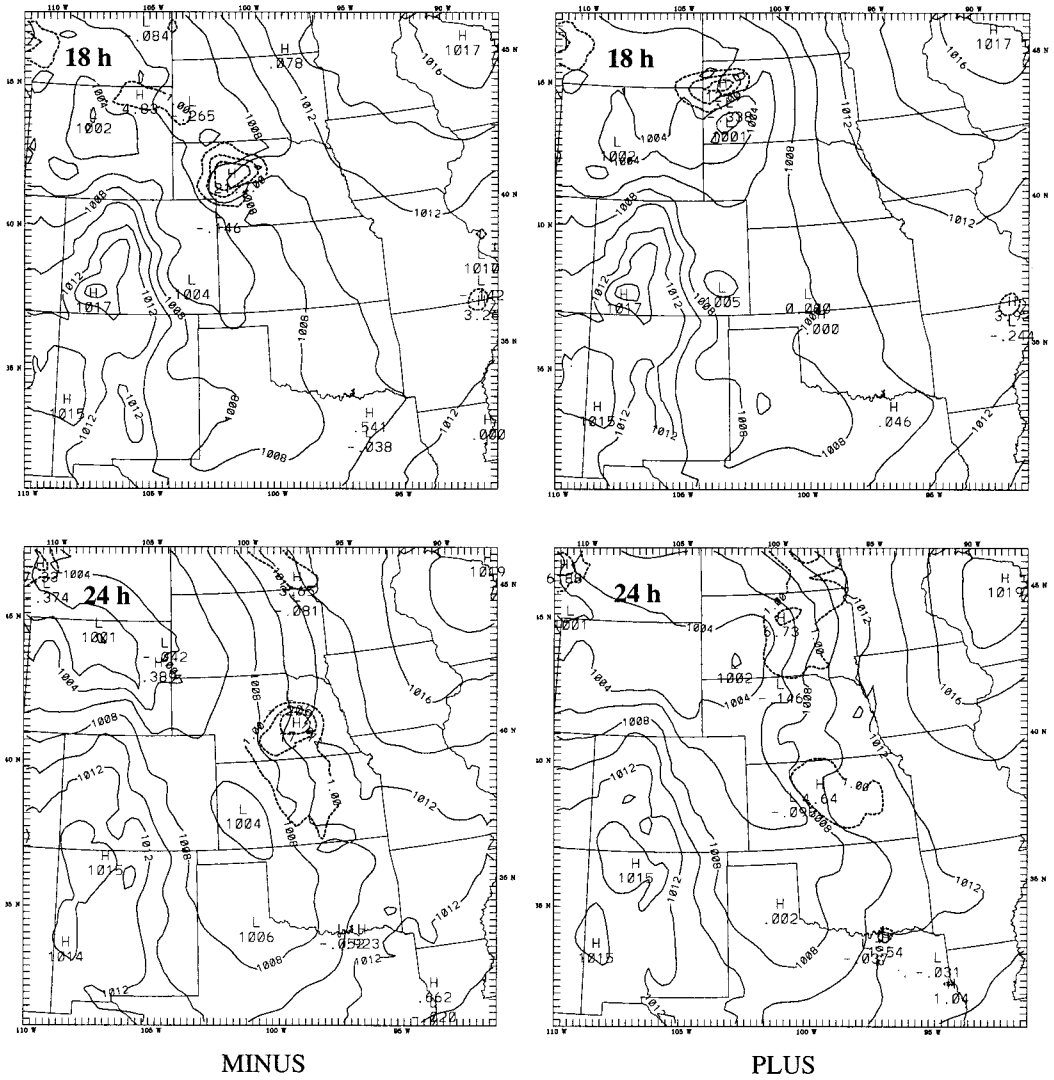

FIG. 12. Modeled 3-h precipitation (mm; dashed) and SLP fields (hPa; solid) from perturbation simulations valid at 18 and 24 h, using initial conditions from experiment J5. (left) MINUS run; (right) PLUS run. The contour intervals are the same as in Fig. 6.

moving MCS becomes much weaker and produces little precipitation after 24 h.

Comparison of the low-level moisture divergence over area A for the two perturbation simulations and the control run shows that the maximum changes again occur at 9 h, the time at which J_5 is defined (Fig. 13). However, the differences from the control persist only until 12 h, after which time it is difficult to distinguish the perturbation runs. The value of J_5 changes by a maximum of 4.5×10^{-7} s^{-1} from the control to the PLUS run, about two to three times its value in the control run.

The differences in the precipitation simulations between the two simulations using perturbation patterns from experiment J5 seem to be much larger than the differences between the two simulations using patterns from J2. This occurs even though the low-level divergence over area A (J_5) differs from the control for only 5 h, whereas the low-level temperature field over area A (J_2) differs from the control for over 15 h (cf. Figs. 5, 13). When a maximum initial wind perturbation of 3–4 m s^{-1} and initial temperature perturbation of ~1–2 K are used, the two J5 perturbation simulations still show large differences from the control run. Thus, it appears that the simulation of MCSs is extremely sensitive to the low-level moisture divergence field, and is less sensitive to the low-level temperature, prior to convective development for this case.

c. Sensitivity of the simulations to low-level temperature over D (J9)

For experiment J9, differences between the two SLP fields are obvious from the early simulation hours, even

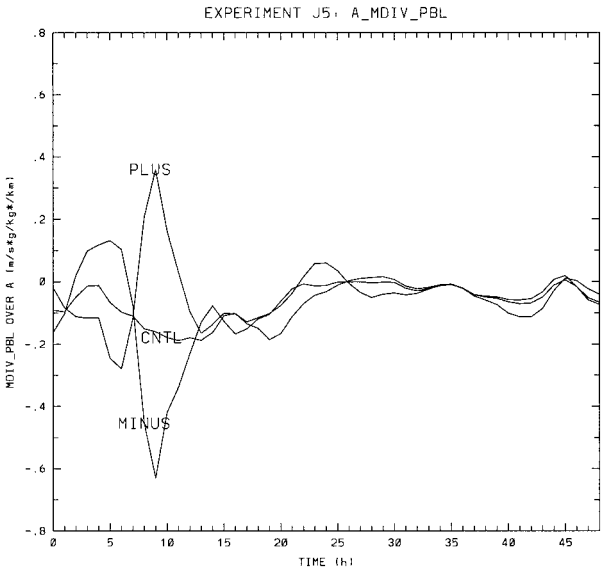

FIG. 13. The response function, PBL moisture divergence (m s^{-1} g kg^{-1} km^1) over area A, as a function of simulation time (h) in the control simulation and the two perturbation simulations using initial conditions from adjoint experiment J5.

though the response function is defined at 18 h. The convective development and evolution in both the perturbed simulations are very different from those of the control simulation (Fig. 14). In the MINUS run, there are two regions of convective activity at 15 h, one in north-central Colorado and another near the Wyoming–Montana border (not shown). The southern system quickly dissipates, while the northern one persists and moves eastward. By 18 h, there is another region of convection in Kansas, which moves southeastward and produces precipitation in Oklahoma between 21 and 27 h. In the PLUS run, there is only one major area of precipitation after 18 h, which is located in northern South Dakota. There is no precipitation in Oklahoma between 21 and 27 h. Results also show that the maximum perturbation in the PBL temperatures over area D is about 2–3 K (Fig. 15). However, in contrast with experiment J2, relatively large changes in PBL temperature are maintained throughout the entire 48-h simulation period.

Changing the 18-h PBL temperature in area D causes a larger difference in the model precipitation after 30 h than changing the 9-h PBL temperature in area A. One interpretation of these results is that the differences caused by perturbing the low-level temperatures at 9 h diminish during the overnight PBL evolution and therefore have less effect on the convective evolution in the later hours of the simulation. A second interpretation is that the PBL structures of the region into which the MCS moves are just as important to the MCS evolution as is the initial strength of the MCS near the time of initiation.

7. Comparison of ensemble generation techniques

Stensrud et al. (2000) examine this same MCS event using two very different methods for generating an identically sized ensemble. One method uses a Monte Carlo approach, developed by Errico and Baumhefner (1987) and modified by Du et al. (1997), to produce 19 different initial conditions for a fixed version of MM5. The other method uses five different convective schemes, two different PBL schemes, and three different moisture availability specifications to produce 19 different versions of MM5 for a fixed initial condition. Results from these initial-condition and physics ensembles indicate that the model physics ensemble is slightly more skillful and produces variance much more quickly than the initial condition ensemble for this case. This highlights the importance of model physics to the creation of ensembles for short-range forecasting, since the different convective parameterization schemes have different criteria for deciding when and where convection develops. These criteria are strongly influenced by the evolution of the PBL, such that feedbacks between the land surface, PBL, and CPSs all contribute to produce variance in the simulations.

The initial condition and physics ensembles reported in Stensrud et al. (2000) are also compared with the adjoint ensemble described herein (see sections 4b and 4c). The purpose of this comparison is to determine whether or not using an adjoint-based approach to the creation of an initial condition ensemble has merit. While we realize that other approaches to automatically producing the ensemble members, such as bred modes (Toth and Kalnay 1997), singular vectors (Palmer et al. 1992), and perturbing the observations (Houtekamer and Derome 1995) may produce results that are different from the Monte Carlo approach used here, we believe that the uncertainties involved in producing ensemble members for short-range forecasting are large enough that our comparisons should be useful. Our intent is not to show the superiority of one method over the other, but to illustrate proof-of-concept for an adjoint-based ensemble approach. In addition, we suspect that forecasters could quickly gain skill in using the adjoint model to develop the ensemble members, leading to better ensembles than we have been able to create.

One method for displaying ensemble data is to calculate the raw ensemble probabilities for specific values of selected model parameters. Since the forecast parameter of most importance for this event is convection, the probability at which the ensemble produces rainfall of 2.54 mm or greater during a specified 6-h period is examined (Fig. 16). Results indicate that the adjoint ensemble fails to produce widespread convection over southeastern Oklahoma during the first 6 h (Fig. 16a). This is not surprising, since the adjoint ensemble is designed to investigate convective development over Wyoming and Nebraska at 9 h into the simulation. However, it is encouraging that some convection does de-

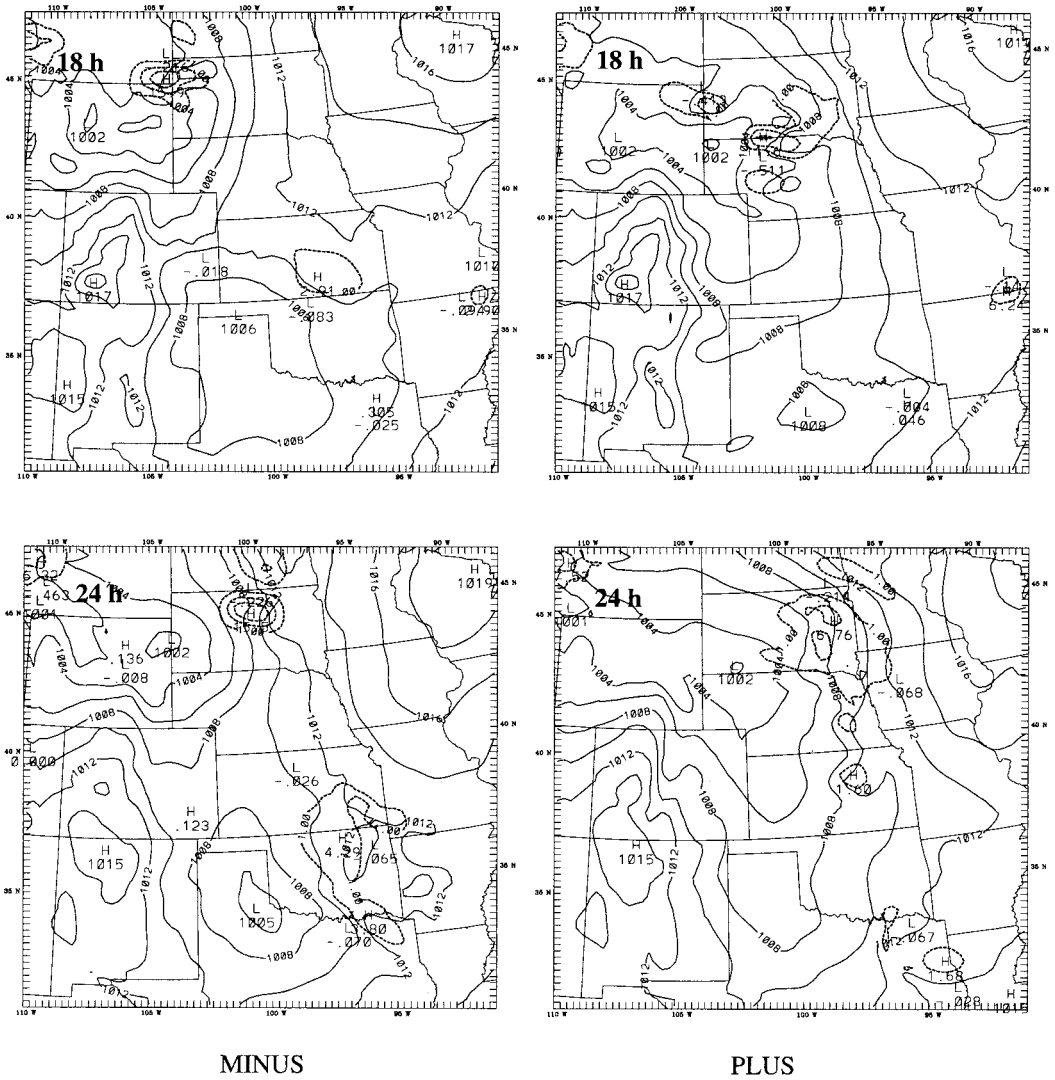

FIG. 14. Modeled 3-h precipitation (mm; dashed) and SLP fields (hPa; solid) from perturbation simulations valid at 18 and 24 h, using initial conditions from experiment J9. (left) MINUS run; (right) PLUS run. The contour intervals are the same as in Fig. 6.

velop over Oklahoma, where the initial condition ensemble produces none (cf. Figs. 7 and 8 in Stensrud et al. 2000).

During the second 6-h period, the adjoint ensemble produces no convection over Oklahoma (Fig. 16b), in agreement with observations, but in contrast with the erroneous continuation of convection in both the physics and initial condition ensembles. While the reasons for this behavior are difficult to determine, this result emphasizes the nonlocal response of a model simulation to incorporating the sensitivity patterns (Errico et al. 1993). This positive modification to the model simulations over Oklahoma is an unintended consequence of the fields chosen for evaluation.

The initiation of convection over southeastern Wyoming is also seen during the first 12 h (Fig. 16b). The probabilities associated with this area of convective development increase during the next 6 h as the region of rainfall shifts eastward into western Nebraska. Two separate regions of rainfall are seen in the ensemble, with one moving northeastward into South Dakota and the other moving southeastward into Nebraska and Kansas by 24 h. According to the adjoint ensemble, either system is equally likely. While the probabilities decrease by 30 h, the ensemble still contains members that replicate the observed convection in Kansas and Oklahoma.

Another method for evaluating the ensemble data is to examine the tracks of the MCS centroids as determined from 3-h precipitation totals (Fig. 17). These are produced by following the centroid of the 5 mm $(3\ \text{h})^{-1}$ rainfall regions. Results indicate that the adjoint ensemble produces much more variance in MCS tracks than does the initial condition ensemble, and has spread similar to that produced by the physics ensemble. While

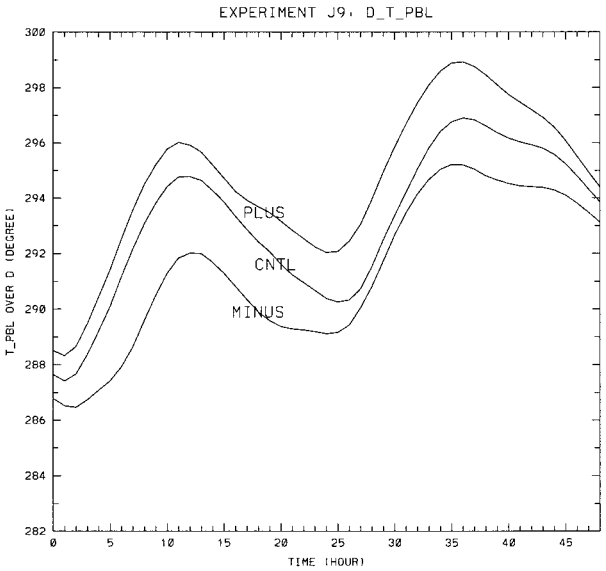

FIG. 15. The response function, PBL temperature (K) over area D, as a function of simulation time (h) in the control simulation and the two perturbation simulations using initial conditions from adjoint experiment J9.

this comparison is more qualitative than quantitative, a resampling method developed by Preisendorfer and Barnett (1983) can be used to quantify these comparisons (see Stensrud et al. 2000 for details). By assigning a value of 1 to each grid point with a 3-h precipitation total of 1.0 mm or greater, and a value of 0 to all other grid points, the area of precipitation is identified without regard to the specific precipitation amounts. These fields of precipitation area are then compared, with results indicating that the adjoint ensemble produces greater variance in precipitation area than the initial condition ensemble and slightly less variance than the physics ensemble (Fig. 18). This result suggests that the adjoint ensemble is able to produce variance in the MCS evolution that is greater than that produced by an automated initial condition generation scheme, and may be a reasonable approach to developing a short-range ensemble.

Calculations of the equitable threat score (ETS; Rogers et al. 1995) from the ensemble mean, after the bias between the forecasts are equalized (see Hamill 1999), and the ranked probability score (RPS; Wilks 1995) indicate that the adjoint ensemble provides a better QPF than either the initial condition or model physics ensembles for the period of 6–24 h, after the MCS has developed and is moving across Kansas (Table 2). While these results are only from one event and need to be corroborated with many other cases, they do suggest that an adjoint-based ensemble generation technique that is constructed by a forecaster has the ability to improve upon automated techniques for generating ensemble members.

If the variance of other variables is examined, then we find that the adjoint ensemble produces less variance than the initial condition and model physics ensembles (not shown). This is not surprising, since the adjoint ensemble is focused upon only one region of the model simulation. However, the variance produced within this region of MCS development and evolution can be substantial and equal that of the other two ensembles for brief periods of time, typically near the time when the sentivitity analysis is valid.

8. Summary and conclusions

Results from the adjoint ensemble, created using output from a set of sensitivity experiments designed by the authors, indicates that it may be beneficial to have a human forecaster involved in the creation of ensembles for short-range forecasting. Past studies show that forecasters routinely improve upon numerical guidance and can identify mesoscale-sized areas of significant severe weather threat with a high level of skill. Through the

TABLE 2. Equitable threat scores (ETS) and ranked probability scores (RPS) from the initial condition (IC), physics (PH), and adjoint (ADJ) ensembles calculated from 6-h precipitation totals valid from 6 to 48 h. To calculate the RPS, we use five categories of 1) no measurable precipitation (pp $<$ 0.254 mm), 2) 0.254 mm $\leq$ pp $<$ 2.54 mm, 3) 2.54 mm $\leq$ pp $<$ 12.7 mm, 4) 12.7 mm $\leq$ pp $<$ 25.4 mm, and 5) pp $=$ 25.4 mm. Values that are significantly different at the 99% level, as tested using the pool-permutation procedure of Preisendorfer and Barnett (1983), with respect to the two other simulations are shown in bold.

	6 h	12 h	18 h	24 h	30 h	36 h	42 h	48 h
ETS: 0.254-mm threshold								
ADJ	0.17	0.17	0.10	0.10	0.16	0.15	0.16	0.19
IC	0.19	0.16	0.09	0.09	0.13	0.13	0.14	0.22
PH	**0.24**	0.12	**0.12**	0.13	0.17	0.09	0.16	0.22
ETS: 2.54-mm threshold								
ADJ	0.15	0.01	0.06	**0.10**	**0.13**	0.0	**0.10**	0.03
IC	0.13	0.0	0.04	0.02	0.04	0.04	0.0	−0.03
PH	0.13	−0.01	0.02	0.03	0.03	0.04	0.06	0.04
RPS								
ADJ	0.712	**0.498**	**0.532**	**0.359**	**0.499**	0.790	0.537	0.576
IC	0.712	0.561	0.585	0.404	0.554	0.796	0.582	**0.402**
PH	**0.625**	0.516	0.548	0.460	0.575	**0.737**	**0.493**	0.449

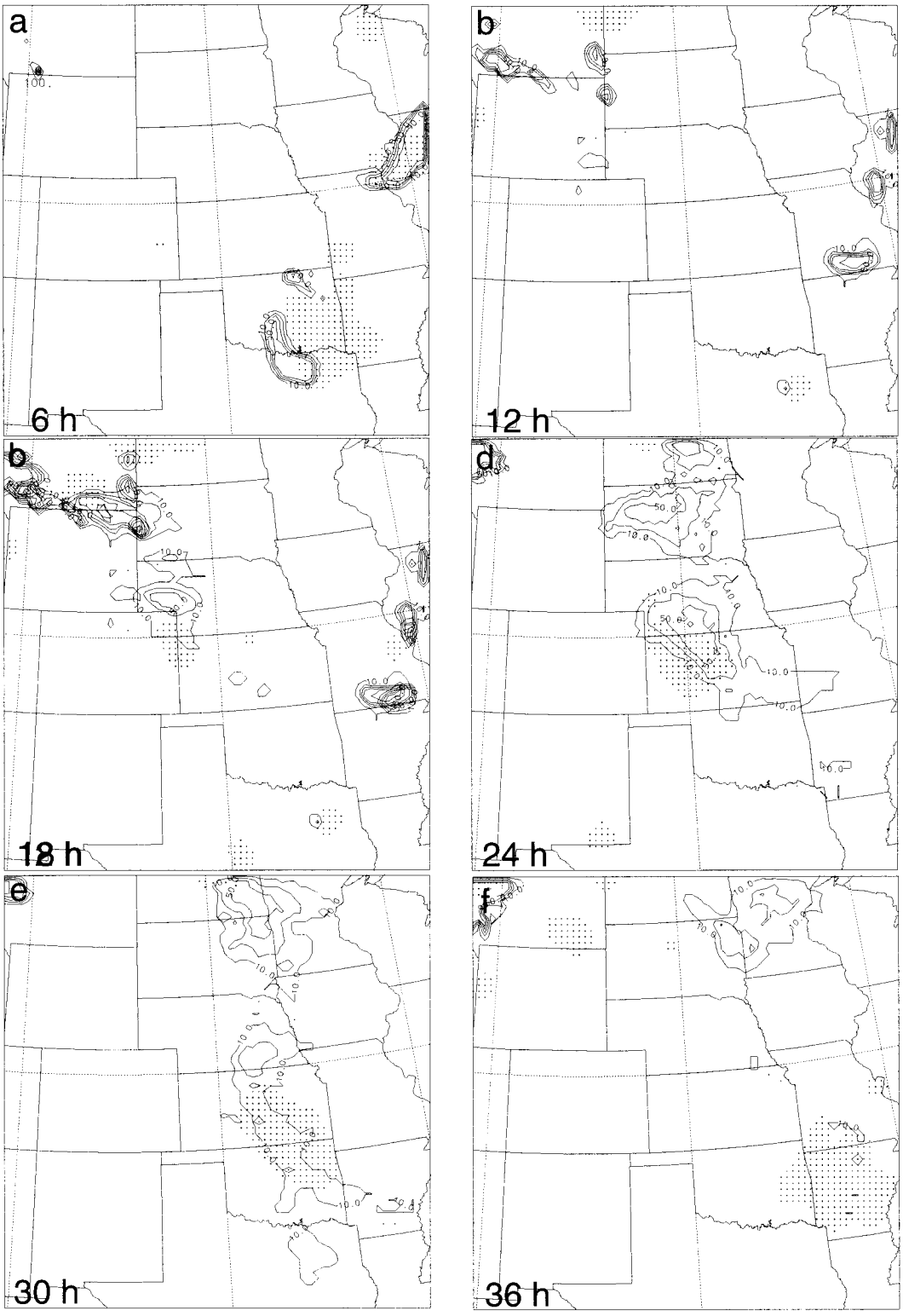

FIG. 16. Probability (expressed in %) of accumulated rainfall = 2. 54 mm from the adjoint ensemble and locations of observed rainfall = 2.54 mm. Plots valid at the (a) 6 h, (b) 12 h, (c) 18 h, (d) 24 h, (e) 30 h, and (f) 36 h simulation times. A contour interval of 20% is used for the probabilities, with the 10% line plotted as well. Observed locations denoted by the points.

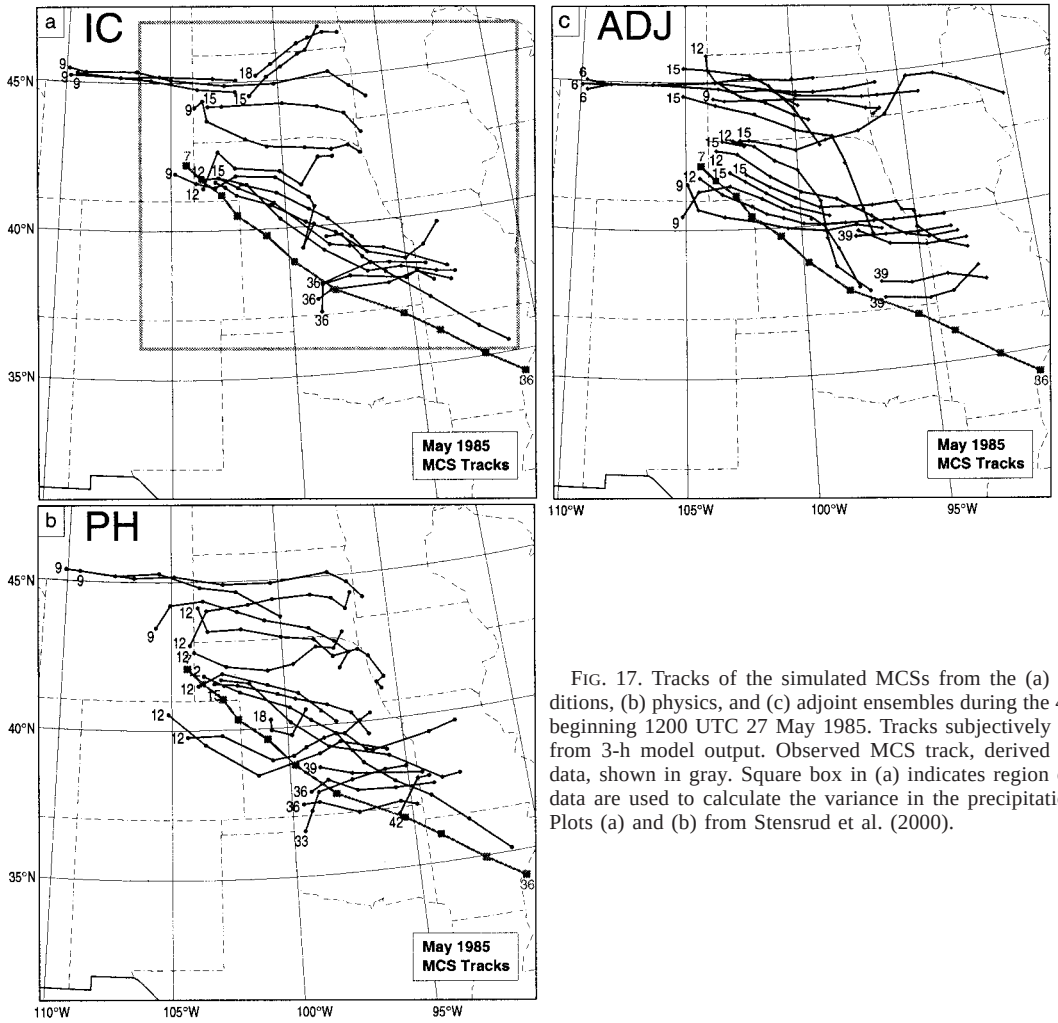

FIG. 17. Tracks of the simulated MCSs from the (a) initial conditions, (b) physics, and (c) adjoint ensembles during the 48-h period beginning 1200 UTC 27 May 1985. Tracks subjectively determined from 3-h model output. Observed MCS track, derived from radar data, shown in gray. Square box in (a) indicates region over which data are used to calculate the variance in the precipitation regions. Plots (a) and (b) from Stensrud et al. (2000).

techniques of parameter evaluation, pattern recognition, and a knowledge of severe weather climatology, forecasters have insights into the daily weather forecast problems that far exceed what can be provided by a numerical weather prediction model alone. It seems logical that some method should be developed to use these insights in the creation of short-range ensemble forecasts in order to better define the possible evolution of the atmosphere on a given day. An adjoint model provides the basis for the development of such a method.

This approach is tested for the 48-h period beginning 1200 UTC 27 May 1985, in which a long-lived MCS develops and moves across Nebraska, Kansas, Oklahoma, and Arkansas underneath a large-scale ridge. While this analysis is conducted only on this one event, this MCS represents a difficult forecast situation that is typical of summertime convective activity in the central United States. A mesoscale adjoint model is used to define the alterations to the model initial conditions necessary to evaluate the influences of key mesoscale structures that we believe have a large influence on later convective development in the model. For this MCS event, two regions of interest are investigated: the region of convective initiation in the control run, and the region into which the MCS moves in the control run. A number of numerical experiments are performed to evaluate the feasibility of using forecaster-selected adjoint sensitivity vectors for ensemble forecasting of MCSs. We believe that operational forecasters would be able to rapidly develop skill in using this type of approach, leading to results that are better than those presented.

Using a simplified adjoint model, we show that the adjoint technique creates a correct directional response in the MM5 simulation. The sensitivity patterns appear to have features that are either related to the large-scale flow or to the small-scale flow, depending on how the response functions are defined. It is clear that our lack of knowledge on the error characteristics of model analyses on the mesoscale is significant and that the perturbation sizes used in this study may be an overestimate. Observational systems that capture the horizontal and temporal evolution of mesoscale atmospheric fea-

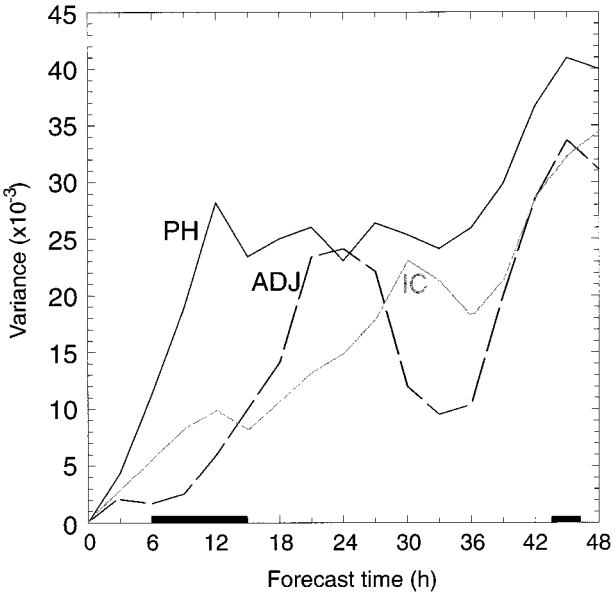

FIG. 18. Variance versus simulation time (h) of precipitation region calculated from the initial condition (IC; gray line), physics (PH; solid line), and adjoint (ADJ; dashed line) ensembles over the region shown in Fig. 17a. Dark lines along the time axis denote time periods in which the differences in the variances (largest compared to second largest) are determined to be significant at the 90% level or greater.

tures are needed if we are to better determine the mesoscale analysis uncertainty for both ensemble and data assimilation applications.

When compared to the initial condition and model physics ensembles of this event, as reported in Stensrud et al. (2000), it is seen that the adjoint ensemble produces more variance than the initial condition ensemble and almost as much variance as the model physics ensemble. This may be due in part to an overestimate of the perturbation sizes used to generate the ensemble members. However, the values of ETS and RPS are better for the adjoint ensemble between 6 and 24 h than for either of the other two ensembles. This result suggests that an ensemble that incorporates the wealth of experience and expertise possessed by forecasters could be a very powerful tool in providing high-quality forecast guidance. It is possible that this adjoint-based technique could be combined with other initial condition perturbation techniques, such as singular vectors, breeding of growing modes, and perturbed observations, and model physics perturbation techniques to produce an even more skillful forecast. Research is needed to determine if this type of approach would be valuable.

Acknowledgments. This study was supported by the National Science Foundation under Grants ATM-9424397 and ATM-9501532. The MM5 and MM5-4DVAR simulations were produced on the NCAR Crays and the support of both NCAR/SCD and NCAR/MMM is deeply appreciated. The Penn State–NCAR mesoscale modeling system is maintained by the efforts of many scientists at both institutions and we are grateful for all their hard work and dedication to making this model easily accessible and user friendly. Reviews provided by Dr. Tom Hamill and two anonymous reviewers are greatly appreciated.

REFERENCES

Anderson, J. L., 1997: The impact of dynamical constraints on the selection of initial conditions for ensemble predictions: Low-order perfect model results. *Mon. Wea. Rev.,* **125,** 2969–2983.

Baer, F., and J. Tribbia, 1977: On complete filtering of gravity modes through non-linear initialization. *Mon. Wea. Rev.,* **105,** 1536–1539.

Bao, J.-W., and R. M. Errico, 1997: An adjoint examination of a nudging method for data assimilation. *Mon. Wea. Rev.,* **125,** 1355–1373.

Barkmeijer, J., 1992: Local error growth in a barotropic model. *Tellus,* **44A,** 314–323.

——, M. van Gijzen, and F. Bouttier, 1998: Singular vectors and estimates of the analysis error covariance metric. *Quart. J. Roy. Meteor. Soc.,* **124,** 1695–1713.

Benjamin, S. G., and N. L. Seaman, 1985: A simple scheme for objective analysis in curved flow. *Mon. Wea. Rev.,* **113,** 1184–1198.

Betts, A. K., and M. J. Miller, 1993: The Betts–Miller scheme. *The Representation of Cumulus Convection in Numerical Models, Meteor. Monogr.,* No. 46, Amer. Meteor. Soc., 107–121.

Blackadar, A. K., 1979: High resolution models of the planetary boundary layer. *Advances in Environmental Science and Engineering,* J. Pfafflin and E. Ziegler, Eds., Vol. 1, Gordon and Breach, 50–85.

Bouttier, F., 1993: The dynamics of error covariances in barotropic model. *Tellus,* **45A,** 408–423.

Brooks, H. E., and C. A. Doswell III, 1993: New technology and numerical weather prediction—A wasted opportunity? *Weather,* **48,** 173–177.

Buizza, R., 1997: Potential forecast skill of ensemble prediction and spread and skill distributions of the ECMWF ensemble predictions system. *Mon. Wea. Rev.,* **125,** 99–119.

——, and A. Montani, 1999: Targeting observations using sigular vectors. *J. Atmos. Sci.,* **56,** 2965–2985.

——, R. J. Barkmeijer, R. Gelaro, and J.-F. Mahfouf, 1996: Singular vectors, norms and large-scale condensation. Preprints, *11th Conf. on Numerical Weather Prediction,* Norfolk, VA, Amer. Meteor. Soc., 50–51.

——, M. Miller, and T. N. Palmer, 1999: Stochastic representation of model uncertainties in the ECMWF ensemble prediction system. *Quart. J. Roy. Meteor. Soc.,* **125,** 2887–2908.

Daley, R., 1979: The application of a nonlinear normal mode initialization to an operational forecast model. *Atmos.–Ocean,* **17,** 98–123.

Doswell, C. A., III, 1987: The distinction between large-scale and mesoscale contribution to severe convection: A case study. *Wea. Forecasting,* **2,** 3–16.

Du, J., S. L. Mullen, and F. Sanders, 1997: Short-range ensemble forecasting of quantitative precipitation. *Mon. Wea. Rev.,* **125,** 2427–2459.

Dudhia, J., 1989: Numerical study of convection observed during the winter monsoon experiment using a mesoscale two-dimensional model. *J. Atmos. Sci.,* **46,** 3077–3107.

——, 1993: A nonhydrostatic version of the Penn State/NCAR mesoscale model: Validation tests and the simulation of an Atlantic cyclone and cold front. *Mon. Wea. Rev.,* **121,** 1493–1513.

Ehrendorfer, M., R. M. Rrrico, and K. D. Raeder, 1999: Singular

vector perturbation growth in a primitive equation model with moist physics. *J. Atmos. Sci.,* **56,** 1627–1648.
Einaudi, F., W. L. Clark, D. Fua, J. L. Green, and T. E. VanZandt, 1987: Gravity waves and convection in Colorado during July 1983. *J. Atmos. Sci.,* **44,** 1534–1553.
Emanuel, K. A., and D. J. Raymond, 1992: Report from a workshop on cumulus parameterization Key Biscayne, Florida, 3–5 May 1991. *Bull. Amer. Meteor. Soc.,* **73,** 318–325.
Eom, J. K., 1975: Analysis of the internal gravity wave occurrence of 19 April 1970 in the midwest. *Mon. Wea. Rev.,* **103,** 217–226.
Errico, R. M., 1997: What is an adjoint model? *Bull. Amer. Meteor. Soc.,* **78,** 2577–2591.
——, 2000: Interpretations of the total energy and rotational energy norms applied to determination of singular vectors. *Quart. J. Roy. Meteor. Soc.,* **126,** 1581–1599.
——, and D. P. Baumhefner, 1987: Predictibility experiments using a high-resolution limited-area model. *Mon. Wea. Rev.,* **115,** 488–504.
——, and T. Vukicevic, 1992: Sensitivity analysis using an adjoint of the PSU–NCAR mesoscale model. *Mon. Wea. Rev.,* **120,** 1644–1660.
——. ——, and K. Reader, 1993: Examination of the accuracy of a tangent linear model. *Tellus,* **45A,** 463–477.
Fiorino, M., J. S. Goerss, J. J. Jensen, and E. J. Harrison Jr., 1993: An evaluation of the real-time tropical cyclone forecast skill of the navy operational global atmospheric prediction system in the western North Pacific. *Wea. Forecasting,* **8,** 3–24.
Fritsch, J. M., and C. F. Chappell, 1981: Preliminary numerical tests of the modification of mesoscale convective systems. *J. Appl. Meteor.,* **20,** 910–921.
Funk, T. W., 1991: Forecasting techniques utilized by the Forecast Branch of the National Meteorological Center during a major convective rainfall event. *Wea. Forecasting,* **6,** 548–564.
Gauthier, P., P. Courtier, and P. Moll, 1993: Assimilation of simulated wind lidar data with a Kalman filter. *Mon. Wea. Rev.,* **121,** 1803–1820.
Gelaro, R., R. H. Langland, G. D. Rohaly, and T. E. Rosmond, 1999: An assessment of the singular-vector approach to targeted observing using the FASTEX dataset. *Quart. J. Roy. Meteor. Soc.,* **125,** 3299–3327.
Goerss, J. S., and R. A. Jeffries, 1994: Assimilation of synthetic tropical cyclone observations into the Navy Operational Global Atmospheric Prediction System. *Wea. Forecasting,* **9,** 557–576.
Grell, G. A., J. Dudhia, and D. R. Stauffer, 1994: A description of the fifth-generation Penn State/NCAR mesoscale model (MM5). NCAR Tech. Note NCAR/TN-398+STR, National Center for Atmospheric Research, Boulder, CO, 122 pp.
Hamill, T. M., 1999: Hypothesis tests for evaluating numerical precipitation forecasts. *Wea. Forecasting,* **14,** 155–167.
Heideman, K. F., and J. M. Fritsch, 1988: Forcing mechanisms and other characteristics of significant summertime precipitation. *Wea. Forecasting,* **3,** 115–130.
Hoecker, W. H., Jr., 1963: Three southerly low-level jet streams delineated by the Weather Bureau special pibal network of 1961. *Mon. Wea. Rev.,* **91,** 573–582.
Houtekamer, P. L., and J. Derome, 1995: Methods for ensemble prediction. *Mon. Wea. Rev.,* **123,** 2181–2196.
——, and L. Lefaivre, 1997: Using ensemble forecasts for model validation. *Mon. Wea. Rev.,* **125,** 2416–2426.
Janjic, Z. I., 1994: The step-mountain eta coordinate model: Further developments of the convection, viscous sublayer, and turbulence closure schemes. *Mon. Wea. Rev.,* **122,** 927–945.
Kain, J. S., and J. M. Fritsch, 1993: Convective parameterization for mesoscale models: The Kain–Fritsch scheme. *The Representation of Cumulus in Numerical Models, Meteor. Monogr.,* No. 46, Amer. Meteor. Soc., 165–170.
Kuo, Y.-H., X. Zou, and Z. Guo, 1996: Variational assimilation of precipitable water using a nonhydrostatic mesoscale adjoint model. Part I: Moisture retrieval and sensitivity experiments. *Mon. Wea. Rev.,* **124,** 122–147.
——, ——, and W. Huang, 1997: The impact of global positioning system data on the prediction of an extratropical cyclone: An observing system simulation experiment. *J. Dyn. Atmos. Ocean,* **27,** 439–470.
Langland, R. H., R. L. Elsberry, and R. M. Errico, 1995: Evaluation of physical processes in a idealized extratropical cyclone using adjoint sensitivity. *Quart. J. Roy. Meteor. Soc.,* **121,** 1349–1386.
——, R. Gelaro, G. D. Rohaly, and M. A. Shapiro, 1999: Targeted observations in FASTEX: Adjoint-based targeting procedures and data impact experiments in IOP17 and IOP18. *Quart. J. Roy. Meteor. Soc.,* **125,** 3241–3270.
Leftwich, P. W., Jr., J. T. Schaefer, S. J. Weiss, and M. Kay, 1998: Severe convective storm probabilities for local areas in watches issued by the Storm Prediction Center. Preprints, *19th Conf. on Severe Local Storms,* Minneapolis, MN, Amer. Meteor. Soc., 548–551.
Lindzen, R. S., and K.-K. Tung, 1976: Banded convective activity and ducted gravity waves. *Mon. Wea. Rev.,* **104,** 1602–1617.
Lorenz, E. N., 1965: A study of the predictibility of a 28-variable atmospheric model. *Tellus,* **17,** 321–333.
McCarthy, D., J. Schaefer, and M. Kay, 1998: Watch verification at the Storm Prediction Center 1970–1997. Preprints, *19th Conf. on Severe Local Storms,* Minneapolis, MN, Amer. Meteor. Soc., 603–606.
Meitin, J. G., Jr., and J. B. Cunning, 1986: The Oklahoma-Kansas preliminary regional experiment for STORM-Central (OK PRESTORM) volume I: Daily operations summary. NOAA Tech. Memo. ERL ESG-20, 313 pp.
Molenti, F., R. Buizza, N. Palmer, and T. Petroliagis, 1996: The ECMWF ensemble prediction system: Methodology and validation. *Quart. J. Roy. Meteor. Soc.,* **122,** 73–119.
Montani, A., A. J. Thorpe, R. Buizza, and P. Unden, 1999: Forecast skill of the ECMWF model using targeted observations during FASTEX. *Quart. J. Roy. Meteor. Soc.,* **125,** 3219–3240.
Mostek, A. J., and N. W. Junker, 1989: Quantitative precipitation forecast verification at the National Meteorological Center. Preprints, *12th Conf. on Weather Analysis and Forecasting,* Monterey, CA, Amer. Meteor. Soc., 633–639.
Palmer, T. N., F. Molteni, R. Mureau, R. Buizza, P. Chapelet, and J. Tribbia, 1992: Ensemble prediction. ECMWF Research Department Tech. Memo. 188, 30 pp. [Available from ECMWF, Shinfield Park, Reading, RG2 9AX, United Kingdom.]
——, R. Gelaro, J. Barkmeijer, and R. Buizza, 1998: Singular vectors, matrices, and adaptive observations. *J. Atmos. Sci.,* **55,** 633–653.
Porter, J. M., L. L. Means, J. E. Hovde, and W. B. Chappell, 1955: A synoptic study on the formation of squall lines in the north central United States. *Bull. Amer. Meteor. Soc.,* **36,** 390–396.
Powers, J. G., and R. J. Read, 1993: Numerical simulation of the large-amplitude mesoscale gravity-wave event of 15 December 1987 in the central United States. *Mon. Wea. Rev.,* **121,** 2285–2308.
Preisendorfer, R. W., and T. P. Barnett, 1983: Numerical model-reality intercomparison tests using small-sample statistics. *J. Atmos. Sci.,* **40,** 1884–1896.
Rabier, F., P. Courtier, and O. Talagrand, 1992: An application of adjoint models to sensitivity analysis. *Beitr. Phys. Atmos.,* **65,** 177–192.
——, E. Klinker, P. Courtier, and A. Hollingsworth, 1996: Sensitivity of forecast errors to initial conditions. *Quart. J. Roy. Meteor. Soc.,* **122,** 121–150.
Reynolds, C. A., R. Gelaro, and T. N. Palmer, 2000: Examination of targeting methods in a simplified setting. *Tellus,* **52A,** 391–411.
Rockwood, A. A., and R. A. Maddox, 1988: Mesoscale and synoptic scale interactions leading to intense convection: The case of 7 June 1982. *Wea. Forecasting,* **3,** 51–68.
Rogers, E., D. G. Deaven, and D. J. DiMego, 1995: The regional analysis system for the operational ''early'' eta model: Original

80-km configuration and recent changes. *Wea. Forecasting,* **10,** 810–825.

Stensrud, D. J., and J. M. Fritsch, 1994: Mesoscale convective systems in weakly forced large-scale environments. Part III: Numerical simulations and implications for operational forecasting. *Mon. Wea. Rev.,* **122,** 2084–2104.

——, G. Manikin, E. Rogers, and K. Mitchell, 1999: Importance of cold pools to mesoscale model forecasts. *Wea. Forecasting,* **14,** 650–670.

——, J.-W. Bao, and T. T. Warner, 2000: Using initial condition and model physics perturbations in short-range ensemble simulations of mesoscale convective systems. *Mon. Wea. Rev.,* **128,** 2077–2107.

Stobie, J. G., F. Einaudi, and L. W. Uccellini, 1983: A case study of gravity waves–convective storms interaction: 9 May 1979. *J. Atmos. Sci.,* **40,** 2804–2830.

Temperton, C., and D. L. Williamson, 1979: Normal mode initialization for a multilevel grid point model. ECMWF Tech. Rep. No. 12, 38 pp. [Available from ECMWF, Shinfield Park, Reading, RG2 9AX, United Kingdom.]

Toth, Z., and E. Kalnay, 1993: Ensemble forecasting at NMC: The generation of perturbations. *Bull. Amer. Meteor. Soc.,* **74,** 2317–2330.

——, and ——, 1997: Ensemble forecasting at NCEP and the breeding method. *Mon. Wea. Rev.,* **125,** 3297–3319.

Uccellini, L. W., 1975: A case study of apparent gravity wave initiation of severe convective storms. *Mon. Wea. Rev.,* **103,** 497–513.

Vukicevic, T., 1991: Nonlinear and linear evolution of initial forecast errors. *Mon. Wea. Rev.,* **119,** 1602–1611.

Wang, W. , and N. L. Seaman, 1997: A comparison study of convective parameterization schemes in a mesoscale model. *Mon. Wea. Rev.,* **125,** 252–278.

Warner, T. T., Y.-H. Kuo, J. D. Doyle, J. Dudhia, D. R. Stauffer, and N. L. Seaman, 1992: Nonhydrostatic, mesobeta-scale real-data simulations with the Penn State University/National Center for Atmospheric Research mesoscale model. *Meteor. Atmos. Phys.,* **49,** 209–227.

Wilks, D. S., 1995: *Statistical Methods in the Atmospheric Sciences: An Introductions.* Academic Press, 46 pp.

Zhang, D.-L., and R. A. Anthes, 1982: A high-resolution model of the planetary boundary layer–Sensitivity tests and comparisons with SESAME-79 data. *J. Appl. Meteor.,* **21,** 1594–1609.

——, and J. M. Fritsch, 1988: Numerical simulation of the meso-β scale structure and evolution of the 1977 Johnstown flood. Part III: Internal gravity waves and the squall line. *J. Atmos. Sci.,* **45,** 1252–1268.

Zou, X., and Y.-H. Kuo, 1996: Rainfall assimilation through an optimal control of initial and boundaryconditions in a limited-area mesoscale mode. *Mon. Wea. Rev.,* **124,** 2859–2882.

——, ——, and Y.-R. Guo, 1995: Assimilation of atmospheric radio refractivity using a nonhydrostatic adjoint model. *Mon. Wea. Rev.,* **123,** 2229–2249.

——, F. Vandenburghe, M. Pondeca, and Y.-H. Kuo, 1997: Introduction to adjoint techniques and the MM5 adjoint modeling system. NCAR Tech. Note NCAR/TN-435+STR, National Center for Atmospheric Research, Boulder, CO, 110 pp.